FINAL REPORT

ON

REMOTE SENSING RESEARCH FOR NASA GRANT NAGW-690

Prepared by

Willard J. Pierson Jr and Winfield B. Sylvester

REMOTE SENSING LABORATORY

The City College of CUNY
Convent Ave. at 138 Street
New York, NY 10031

May 1995

TABLE OF CONTENTS

PREFACE

This is the final "Final Report" for NASA Grant NAGW-690. This support began on December 1986 and ended on April 1995. Fortunately, limited funding from the Jet Propulsion Laboratory has allowed the continuation on a part time basis of our research efforts for NSCAT and ERS-1 until December 1995.

This final report summarizes the research on model functions for ADEOS and ERS-1 and provides an analysis of the differences between three kinds of models. The success of the AMI on ERS-1 obtained at GSFC and NMC is highlighted. Predictions that were made prior to the receipt of an ESA Contractor Report are verified by that report.

The problem of describing the wind stress is reviewed.

A scatterometer model for high winds for the AMI on ERS-1 and ERS-2 is under development. The present status of this research is described.

Finally, the accomplishments over the years of our past research are reviewed in terms of many published papers that were "firsts" toward the development of the methods used in theories that describe the winds, the waves and the development of the active microwave systems presently operational and planned for spacecraft.

As this final report shows, there is much more that still needs to be done. How and when it will be done and who will do it remain to be decided.

THE PRESENT STATUS OF BACKSCATTER MODELS

The Model Function Subcommittee

A major effort during the past two years has been to contribute portions of the text of the document being prepared by the model function sub-committee which is charged with recommending the preliminary version of the "Model Function" (*Long,* 1995) to be used when NSCAT on ADEOS is placed into orbit. The portions of that report provided by us pointed out various problems that arose in the development of the model function for the SEASAT scatterometer (SASS). The document entitled "Current Progress in Ku-Band Model Functions" prepared by means of contributions from the model function subcommittee and dated 1 May 1995 has been released along with a letter from the subcommittee chairman, David Long. It has been circulated to the full science team. Many of the contributions that we prepared have been included, but many others contributions were not. The report has many parts that need clarification and other parts that need corrections. Comments will be provide to Professor Long during the next few months.

Many of these problems were documented by the research of Peter Woiceshyn in collaboration with Morton Wurtele. Since Mr. Woiceshyn was not a member of the model function committee, it was necessary to describe these results in considerable detail. For example, the results of Woiceshyn and Wurtele showed that there was a systematic concentration of wind directions near the upwind pointing direction for one of the antennas for some ranges of wind speed and incidence angles. For other ranges of incidence angles, the wind directions were concentrated at 45° between upwind and crosswind. Also for some wind speed and incidence angles there were systematic biasses in wind speed. These effects plus our own research indicated that picking a model to be used and an algorithm based on the maximum likelihood estimate plus assorted interpolation schemes

might be premature. The data from NSCAT should be analyzed very carefully to be sure that the best possible model is used before the data are released.

The best possible model for NSCAT does not yet exist, and the present methods for developing one when data become available are not adequate. Unless great care is taken, the model will not be good for light winds and calms and winds over about 17 m/s. Our research, as described below, for the C-Band scatterometer on ERS-1 shows that it ought to be possible to obtain a model for winds as high as 27 m/s.

Present C-Band Analytical Models

The research done on the model function for the C-band scatterometer on ERS-1 illustrated both the success and the failure of the methods that have been used. In our opinion, none of the proposed model functions is optimum. The published papers on the models contradict each other and disagree substantially outside of the range of moderate wind speeds. Very high winds are not modeled correctly. The backscatter values for light winds are incorrect because of the way the data were processed before they were released.

To illustrate the wide variation in the properties of the analytical functions that attempt to relate wind speed to backscatter for C-Band a simplified summary of some of them follows without naming the models.

1) The first model is a power law model of the form

$$\log \sigma^{o}_{1} = \log A_1 + B_1 \log V \qquad (1)$$

or $$\sigma^{o}_{1} = A_1 \, v^{B_1} \qquad (2)$$

for, say, upwind the graph of this model on a double log plot is a straight line for a fixed incidence angle. If the wind speed is zero, the backscatter is zero.

2) The second model in simplified terms, for at least one version, can be represented by

$$\log \sigma^\circ_2 = \log A_2 + B_2 \sqrt{v} \tag{3}$$

$$\text{or} \quad \sigma^\circ_2 = A_2 \; 10^{B_2 \sqrt{v}} \tag{4}$$

The backscatter equals A_2 if the wind speed is zero.

3) The third model has no convenient analytical expression but its behavior relative to the other two can be described.

$$\sigma^\circ_3 = \sigma^\circ_3(V, V_T) \tag{5}$$

The backscatter equals zero if $V = V_T$.

All three of these models can be made to agree at two points when σ° is plotted as a function of v. If then

$$\sigma^\circ_1 (v_1) = \sigma^\circ_2 (v_1) = \sigma^\circ_3 (v_1) \tag{6}$$

and $$\sigma^\circ_1 (v_2) = \sigma^\circ_2 (v_2) = \sigma^\circ_3 (v_2) \quad \text{for} \quad V_1 < V_2 \tag{7}$$

These three models then have the property that:

$$\text{For} \quad v < v_1; \quad \sigma^\circ_2(v) > \sigma^\circ_1(v) > \sigma^\circ_3(v) \tag{8}$$

$$\text{For} \quad v_1 < v < v_2; \quad \sigma^\circ_2(v) < \sigma^\circ_1(v) < \sigma^\circ_3(v) \tag{9}$$

$$\text{For} \quad v_2 < v; \quad \sigma^\circ_2(v) > \sigma^\circ_1(v) > \sigma^\circ_3(v) \tag{10}$$

Each model can in principle be fitted over the limited range for v_1 to v_2, say 5 to 15 m/s. However, if any one of the three should prove to be correct the other two will not yield good results

for low and high wind speeds.

The difficulty with this approach for a model to relate backscatter to wind speed is that once the functional form is chosen, the process of fitting the function to the data cannot change that functional form and the results may fail outside of the range wherein most of the data lie.

Figures 1 and 2 are schematic graphs for these three different models. Figure 1 is for linear scales. Since most data for winds fall in the 5 to 15 m/s range, it is very difficult to discriminate one model from another. For both higher and lower wind speeds, the three models diverge but nevertheless all three predict increasing backscatter with increasing wind speed.

Figure 2 illustrates the difficulties of working in log space, especially for low winds. Model 1 predicts a backscatter value of 0.01 for a wind near one millimeter per second, Model 2 predicts a backscatter value of about 0.012 for no wind. Model 3 predicts a backscatter value of 0.001 for a wind of 2 m/s.

The Success of ERS-1

The value of scatterometer data has been conclusively demonstrated by some unpublished results of Robert Atlas of GSFC and by the development of a method for the routine assimilation of AMI data from ERS-1 into numerical analysis procedure at the National Meteorological Center. The data from ERS-1 are good enough to be useful on a day to day basis from a moderate range of wind speeds.

During the NSCAT meeting in Hawaii, Robert Atlas showed the value of ERS-1 data in many ways. Low pressure centers were found that were not located by conventional data. Those that were located by conventional data were frequently not placed in the correct location. An initial

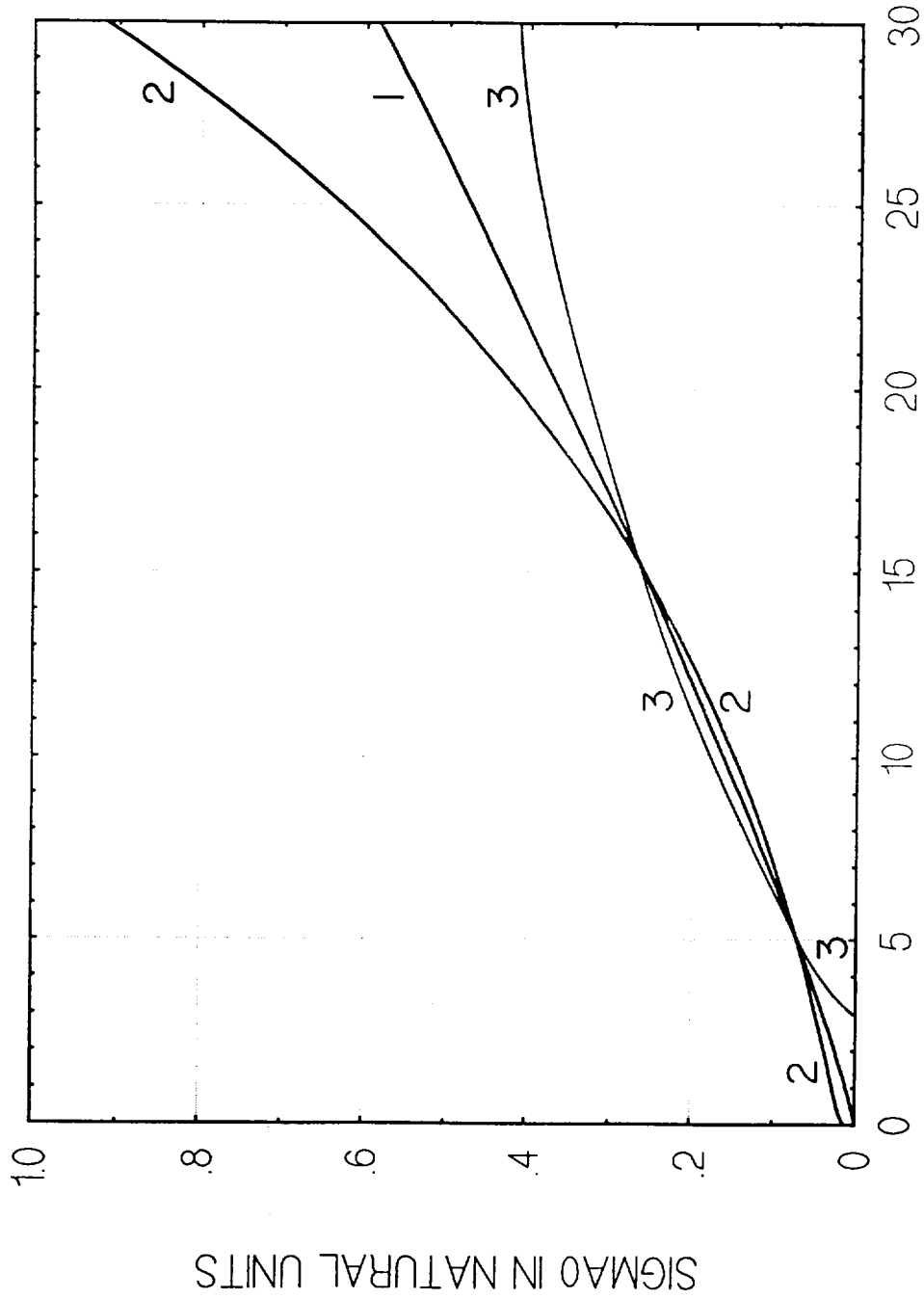

FIGURE 1. SCHEMATIC UPWIND GRAPHS FOR THREE CMOD MODELS

FIGURE 2. DOUBLE LOG PLOT FOR THREE MODELS

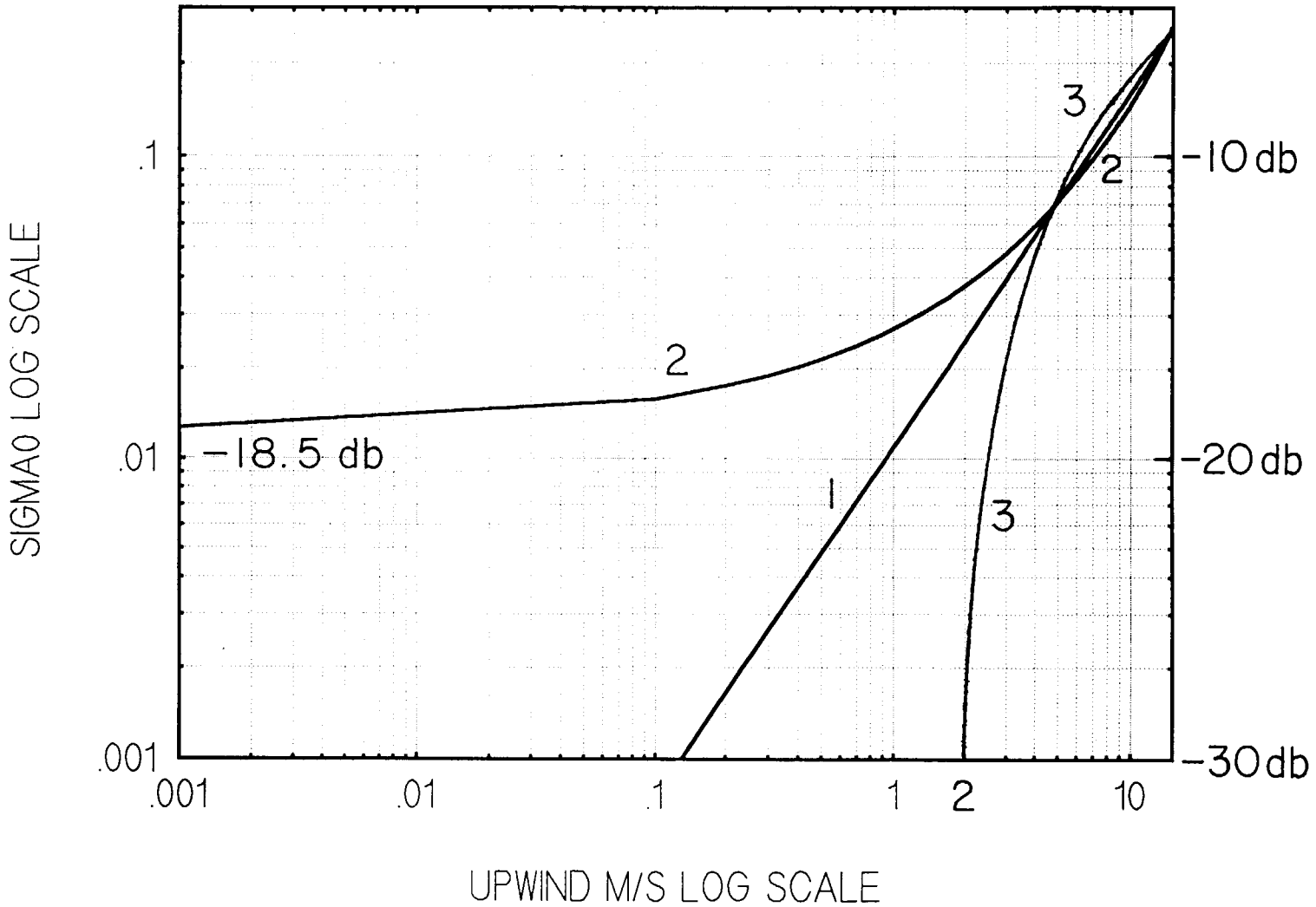

value update for a forecast can not yield a good forecast if it is incorrect. Atlas showed that the range of accuracy of a forecast could be extended by means of ERS-1 data.

Gemmill, et al. (1994) developed a way to intercompare six different model functions for the AMI on ERS-1. They were CMOD 4 from ECMWF, CMOD 5I from IFREMER, CMOD 5L from ESA (the European Space Agency) CMOD 6 from the University of Hamburg, CMOD 7 from NASA-JPL/OSU and ESA (CMOD 4) the ESA "fast delivery product". The model, CMOD 4, is a modification of the CMOD 4 used for the ESA fast delivery product.

The six candidate model functions were compared in terms of objective scores by which the models can be ranked. This procedure does not necessarily mean that a better model cannot be found. In fact, it is already known that the one selected does not yield realistic values for high winds. There is the danger that in the rush to produce results those that are released may be misinterpreted.

Tables 3b, 4b, 5b, 6, and 7b from Gemmill, et al. (1994) rank the statistics obtained by using these six models for a year of data and comparing their winds to data buoy measured winds. For example, for Table 3b, CMOD 5I had the lowest speed bias, ESA had the lowest RMS speed difference, CMOD 5I had the largest speed bias - and so on.

The grand sum given above Table 3b shows that CMOD 4 and CMOD 5I are virtually in a tie and that the other contenders are far behind.

On the basis of this study, the ERS-1 data are being routinely processed at the ocean products center of the National Meteorological Center as described by Peters, et al. (1994). One can confidently expect that an impact of these data will be demonstrated in due course.

GRAND	CMOD4	CMOD5I	CMOD5L	CMOD6	CMOD7	ESA
SUM	51	49	109	127	125	116

Table 3b
TRANSFER FUNCTION RANKINGS

NDBC and TOGA buoys, High Seas, All Data
Space Box: 0.5 degree, Time Window: +/- 3 hours
Dates 93 09 09 - 94 09 09

	CMOD4	CMOD5I	CMOD5L	CMOD6	CMOD7	ESA
SPD BIAS	2	1	6	5	4	2
SPD RMS	2	2	6	4	5	1
SPD COR	3	1	2	6	3	3
DIR RMS	1	2	3	4	5	6
VECT CORR	2	1	3	3	3	6
FOM	1	2	3	4	5	6
SUM	11	9	23	26	25	24

Table 4b
TRANSFER FUNCTION RANKINGS

NDBC Mid-latitude, High-Seas, Winter Data
Space Box: 0.5 degree, Time Window: +/- 3 hours
Date 93 11 01 - 94 04 31

	CMOD4	CMOD5I	CMOD5L	CMOD6	CMOD7	ESA
SPD BIAS	1	3	5	5	5	1
SPD RMS	1	1	5	4	5	1
SPD CORR	2	1	2	6	4	4
DIR RMS	3	1	1	4	5	6
VECT CORR	2	1	2	5	2	6
FOM	1	2	3	3	5	6
SUM	10	9	18	27	26	24

Table 5b
TRANSFER FUNCTION RANKINGS

NDBC Mid-latitude, High-Seas, Summer Data
Space Box: 0.5 degree, Time Window: +/- 3 hours
Date 93 09 09 - 93 10 31 and 94 05 01 - 94 09 09

	CMOD4	CMOD5I	CMOD5L	CMOD6	CMOD7	ESA
SPD BIAS	2	1	5	4	4	2
SPD RMS	1	1	5	4	6	1
SPD CORR	2	1	2	6	3	3
DIR RMS	1	3	1	4	5	6
VECT CORR	1	1	4	3	4	6
FOM	1	1	3	3	5	6
SUM	8	8	20	24	27	24

Table 6b
TRANSFER FUNCTION RANKINGS

TOGA Tropical, High-Seas, Winter Data
Space Box: 0.5 degree, Time Window: +/- 3 hours
Date 93 11 01 - 94 04 31

	CMOD4	CMOD5I	CMOD5L	CMOD6	CMOD7	ESA
SPD BIAS	3	1	5	6	4	2
SPD RMS	3	2	5	6	4	1
SPD CORR	3	1	3	6	2	3
DIR RMS	1	2	3	4	5	6
VECT CORR	2	1	4	5	3	6
FOM	1	2	3	5	4	6
SUM	13	9	23	32	22	24

Table 7b

TRANSFER FUNCTION RANKINGS

TOGA Tropical, High-Seas, Summer Data
Space Box: 0.5 degree, Time Window: +/- 3 hours
Date 93 09 09 - 93 10 31 and 94 05 01 - 94 09 09 4

	CMOD4	CMOD5I	CMOD5L	CMOD6	CMOD7	ESA
SPD BIAS	1	4	5	5	3	1
SPD RMS	2	3	6	5	4	1
SPD CORR	2	2	4	6	4	1
DIR RMS	1	2	2	4	5	6
VECT CORR	2	1	5	3	3	6
FOM	1	2	3	3	6	5
SUM	9	14	25	26	25	20

The ESA Contractor Report

The report by *Stoffelelen and Anderson* (1995) reached us after most of the material in this final report had been written. The material in that report substantiates the statements made above and verified the need for a model for wind speeds over about 15 m/s.

The notation, MLE, originally proposed by *Pierson* (1989a, 1989b) is used, as in Eqn. (1.4) of the report for $K_P = 0.05$ approximately. Actually K_P is a function of three parameters α, β and γ and can be very large for low winds. The parameters α, β and γ have never been defined for ERS-1.

Figure 3.13 in the ESA report reveals two of the difficulties with scatterometry. Both the ECMWF wind field analyses and the scatterometer winds do not identify calms separately. Both plots show no wind speeds above 21 m/s. Both features do not correspond to reality.

Figures 3.16a and 3.16b compare the winds from CMOD4 to the ECMWF winds from a boundary layer model for the Braer Storm. Comparisons of boundary layer model winds, unless great care is taken, are found to be too low when compared to winds measured by a data buoy. Thus the wind speeds in both of these analyses are too low. Nevertheless, the CMOD4 winds are systematically lower than those for the boundary layer analysis.

Similar results are shown for a storm that occurred on 14 March 1993 in figures 3.17a and 3.17b. The ECMWF analysis shows winds of 50 knots (+/-) over a large area, whereas the CMOD4 winds show 40 knots. Again both winds are probably too low.

A graph of CMOD4 at upwind for various incidence angles would differ by modest amounts from the graph for curve 2 in Figure 1. To recover wind speeds of 25 to 30 m/s would require backscatter values that are much too high and that do not occur for these wind speed.

Our preliminary analysis of the Braer Storm attempts to fit power laws similarly to curve 1 in Figure 1 for the wind speed range above about 15 to 20 m./s.

WIND STRESS

The nonlinear equations that describe turbulence in the planetary boundary layer are just as complicated as those that describe water wave properties and perhaps even more so. Attempts to parameterize the stress of the wind on waves and swell have been frustrated by the complexity of the problem.

This was one of the objectives of our research during the past few years. No definitive solution has been obtained. The "Model Function Subcommittee" has recommended that the effective neutral wind at 10 meters be used because this value is not too sensitive to the assumed equation for the stress. The boundary layer models for computer based numerical weather prediction also do not seem to be very sensitive to the choice of a model for the stress.

With the successful deployment of TOPEX/Poseidon, the need for a correct parameterization of the wind stress becomes important so that ocean currents can be modeled.

Many of the efforts to parameterize wind stress in terms of the time averaged wind speed at 10 m have determined the values of A and B in $(U_*^2/\bar{U}(10))^2 = A + B\,\bar{U}(10) = C_{DN}$ with the result that the literature contains values for these two "constants" that differ be large amounts. The reason for these large differences may well be the lack of homosecidity, i.e., representative accurate values of the required data including a full range of wind speeds and wave conditions as defined by wave spectra.

Three important papers on this subject are those of Donelan (1982), Donelan (1990) and Blake (1991). Donelan (1982) stratified wind stress values versus wind speed and wave conditions for short steep waves and longer less steep waves for the same wind speed ranges. The drag coefficient was higher for the same wind speed for the short steep waves than for the longer less steep waves. This showed that wave conditions had to be considered in a model for the wind stress.

Donelan (1990) reviewed the subject and used dimensionless variables based on the Buckingham PI theorem to find a relations between waves, winds and the wind stress.

Blake (1991) used three different sources of data and found that the data from Smith (1980, 1988) could be used to relate the stress to both wind speed and wave height. A copy of this paper is appended to this report.

An important result of Blake was to use drag coefficients proposed by each author on the data for that author and the data for the other two authors. The proposed drag coefficient did well for the data on which it was based, but not on the other two independent data sets. Thus the three data sets lack homosecidity and the data are mutually incompatible.

Our opinion is that the results of Blake need to be pursued further and that they would provide a useful relationship for the wind stress as a function of wave height and the wind at 10 meters.

Advancing technology may make it possible to do a definitive experiment similar to the work of Smith. The directional wave spectrum, the atmospheric stratification, the actual wind stress, a time history of the variables and various other essential parameters will need to be measured at a number of different locations for a year or more as to obtain a homogeneous data base representative of the full range of variability of the quantities involved.

A SCATTEROMETER MODEL FOR HIGH WINDS

Introduction

The complete description of the variables that link σ^0 with the vector wind at the surface of the ocean has yet to be determined. Each model function that now exists as described in simplified terms in a previous section tries to emphasize the suitability and the importance of particular variables that connect σ^0 to the vector wind. Empirically, $\sigma^0 = f(V, \chi, \theta, ...)$ where V is the wind speed, χ the relative azimuth, θ the incidence angle and the ... are all the other known and unknown variables that might be involved.

Scientists must work towards establishing as complete as possible a list of these variables that when put in their right combination should produce the long awaited results that scatterometry has made boast of earlier. In a more practical sense, there is the need of scientists to understand better the basic functional form of the relationship between the electronically measured radar cross-section σ^0 and the wind velocity in space and time. A simplified relationship between σ^0 and V will introduce a "user-friendly" atmosphere among users of marine surface wind products. As part of a negative commentary, the following observation is noted. Operational forecasters are just beginning to make prognostications of modern weather phenomena with the use of scatterometry as a method of data enhancement and/or correction. One of the manifest functions of providing scatterometry winds is to help weather forecasters and ocean modelers in setting up the most accurate and complete data base to study geophysical systems.

Operational remote sensing of real-time winds are just beginning. The data that are utilized do well over a moderate range of wind speeds, but numerous publications have shown that winds above about 15 m/s are not correctly described.

To obtain the surface wind at a height of 10 m above the ocean surface from scatterometry requires a set of logistics to be in place. These are a number of co-located σ^0 values of the ocean surface from at least three viewing geometries and a model function that gives a correct mapping of the radar cross-section parameter to the field of motion. The wind vector is the by-product of this experiment. It is well-documented that if the magnitude portion of the vector can be obtained, then the directions can also be worked out by making use of varying radar viewing geometries and other available data, for example, isobaric and streamline analyses of existing weather maps.

Given the state of the art in electronic engineering, scientists have placed substantial confidence in the backscattered σ^0 values that are received and processed from polar orbiting satellites. Skill in data management and analysis help researchers to find colocated measurements of σ^0 . The somewhat illusive model function continues to make the wind retrieval task both complex and difficult. Scientists are, however, encouraged by some partial results that are obtained from their work with many of the existing model functions. This approach using the method of synthesis has, unfortunately, placed scientists short of the mark. What is needed is an accuracy (within specified limits) that allows the wind output to be usable in operational and research situations. Thus there is evidence that existing model functions need refinement. As is documented, some of them work fairly-well in the mid-range (5 - 15 m/s) of wind speeds. The low and high wind regime ends are much more problematic. Here is the suggestion that there may be other parameters that are important in these parts of the wind spectrum, that are, until now, not included in the formulation. The role of sea-surface temperature at the low end, and spilling waves and breakers at the high end are parameters to be considered. Then there is the question of the limitation of the models themselves.

Our research goals over the past few years have been directed along rather practical lines. Some of the short-comings that have been cited earlier in this report are being addressed. Efforts were concentrated on evaluating and comparing model functions. (See *Sylvester* 1984, *Sylvester et al.* 1989, 1990). Studies of this nature provide an understanding of the pros and cons of certain model functions.

Most of the evaluation techniques are related to self-consistency. Models should be verified against conventionally obtained winds that define the range of speeds obtained over the ocean. For the past two years, efforts have been centered on providing a suitable network of conventionally measured surface winds to be used as a basis for verification, and in particular, winds in excess of 20 m/s. Products from ERS-1 should be verified against high winds so that the validity of model function can be attested.

A further motivation for our approach was based on the following ideas.

* It is known that nature produces high winds over the ocean but the ability to measure them is greatly reduced because many ships generally avoid areas of storms.

* Absolute confidence cannot be placed on winds obtained by ships as pointed out by Pierson (1990).

* Most of the data buoys that provide the best wind products are placed in selected near-shore areas and may not lie in the path of the storm which is the subject of the inquiry.

The project ***IN SEARCH OF HIGH WINDS*** came into existence in 1993. As conceived, it was intended to solve the important problem of finding suitable winds against which model functions could be tested and also to verify the capability of the instrument on ERS-1 as to its wind measurement capability. As pointed out before, obtaining a vector wind field by conventional means

proved prohibitive. The next best method was to resort to the use of corrected synoptic weather maps from which a wind field could be established.

Three NMC synoptic maps became available in the middle of 1993. The deepest and probably the most intense extratropical cyclone in the North Atlantic in this century has to be something worthy of study. Firstly, all additional data relating to the storm had to be obtained before reanalysis could be done and then the utilization of PBL models for obtaining the winds from the pressure field should follow. Finally, the problem of working with scatterometer data in obtaining a model function could be addressed. The description of the methodology of carrying out the analysis of a high wind case is detailed below.

The research sought to provide a network for verifying winds obtained with remote sensors by using the correct pressure field and exploiting the known relationship between the pressure and the wind.

Motivation

1. There are a minimum of errors in the reported pressure field in synoptic maps for the North Atlantic and elsewhere.
2. Synoptic weather maps for the North Atlantic produced by different meteorological offices tend to have good agreement. Where differences exist, reanalysis by the researcher can quickly correct the situation, especially, if more data become available.
3. A "best" pressure map can be produced by merging data sets and map sets. This final map holds the input for the calculation of the wind.

4. The known relationship between pressure and wind and the effect of warm and cold air advection are then utilized. For example, the geostrophic and the gradient winds can be obtained from the pressure fields.

Method and Material

1. Obtain synoptic analyses for NMC and ECMWF plus any other synoptic data made available after map time.
2. Compare products, correct data where necessary, and merge analyses and so as to produce a "final" reanalyzed pressure field.
3. Obtain sea surface temperature fields. In this case, climatology may be sufficient.
4. Calculate wind from PBL models using pressure gradients and air-sea temperature differences as the main inputs.
5. Blend the derived 10-meter winds with the existing buoy and corrected ship data to establish a vector wind field.
6. Carry out the intercomparison between remotely sensed model winds from scatterometry and those obtained from analysis just described above.

PBL Models

The calculated winds are obtained by utilizing the models of *Cardone* (1969, 1978) and the University of Washington (UW) (*Brown and Liu* 1982).

a) A marine PBL model proposed by Cardone calculates the wind speed and in flow angle at anemometer height above the sea surface. In particular, the ratio of the anemometer level wind speed to the geostrophic wind speed and the angle between the surface wind direction and the surface isobars are calculated. This baroclonic, stability-dependent marine boundary layer model has been in operation since the 1970's. It is utilized internationally to obtain winds over the ocean. Table 1 is an example of an output for latitude 50° N for the Cardone model. The table gives the wind speed (first row) and the inflow angle (second row) for an isobaric spacing of 4 mb and air-sea temperature differences as exhibited therein.

However, the following important features as illustrated by *Pierson* (1978) will be included in the model. These are:

(i) the effect of a cold low in increasing cross-isobaric flow for the surface wind;

(ii) the effect of a cold low in increasing the speed of the surface wind;

(iii) the effect of warm air advection in decreasing cross-isobaric flow for the surface wind.

b) The University of Washington (UW) PBL model uses sea level pressure and temperature fields as input.

This is a similarity model that incorporates stratification, variable surface roughness and thermal wind within it.

Products from both models will be intercompared. Greater confidence will be placed in areas where there is good agreement. Where the two models disagree markedly, dynamic criteria will be adopted to decide which model will be followed. The one chosen must establish confirmity with

TABLE 1. Wind Speed in Knots and Inflow Angle as a Function of Air Sea Temperature Difference and the Pressure Gradient. (Cardone Model).

LAT = 50 ISOBAR SPACING 4MB DTX = 0.000000 DTY = 0.000000								
DIFINT >> SPACE DEG. LAT	-16	-8	-4	-2	0	1	2	4
0.250	113.0 15.1	109.2 15.3	106.1 15.6	103.9 15.9	100.4 16.4	96.9 16.9	93.5 17.4	87.0 18.0
0.375	83.6 14.3	80.5 14.5	78.0 14.8	76.1 15.1	72.8 15.8	69.3 16.5	65.9 17.1	59.7 17.7
0.500	67.1 13.7	64.5 14.0	62.4 14.3	60.7 14.6	57.6 15.4	54.6 15.4	50.7 16.9	45.0 17.4
0.625	56.4 13.3	54.2 13.5	52.3 13.8	50.8 14.2	47.9 15.1	44.4 16.1	41.1 16.9	35.9 17.1
0.750	48.9 12.9	46.9 13.2	45.2 13.5	43.9 13.8	41.1 14.8	37.6 16.1	34.4 16.8	29.8 16.7
.0875	43.3 12.7	41.5 12.9	40.0 13.2	38.7 13.6	36.1 14.6	32.6 16.0	29.5 16.7	25.4 16.4
1.000	38.9 12.4	37.3 12.7	35.9 13.0	34.7 13.3	32.2 14.4	28.7 16.0	25.8 16.6	22.2 16.0
1.250	32.5 12.0	31.1 12.3	29.9 12.6	28.9 12.9	26.6 14.2	23.1 16.0	20.4 16.5	17.6 15.4
1.500	28.1 11.7	26.8 12.0	25.3 12.3	24.9 12.6	22.7 13.9	19.3 16.0	16.8 16.3	14.5 15.0
1.750	24.8 11.5	23.6 111.7	22.7 12.0	21.9 12.4	19.8 13.8	16.4 16.1	14.2 16.2	12.3 14.7
2.000	22.2 11.3	21.2 11.5	20.3 11.3	19.5 12.2	17.6 13.7	14.2 16.2	12.2 16.1	10.7 14.5
4.000	12.4 10.6	11.8 11.1	11.2 11.4	10.7 11.3	9.2 14.0	6.4 17.0	5.5 15.7	4.9 13.8
8.000	6.9 11.7	6.5 11.9	6.1 12.2	5.8 12.6	4.7 15.4	2.8 17.2	2.5 15.2	2.2 13.2

DIFINT = Air Sea Temperature Difference

Space Deg. Lat. = Pressure Gradient.

meteorological continuity.

The Braer Storm

The Braer Storm is an example of a suitable data set.

A well-developed cyclone or storm may persist for several days. The intensity and direction of the wind are diagrammed on isobaric maps. Strong winds are associated with large gradients, and from one synoptic map-time to another, the steadiness with which the wind blows can be noted. It is rather common to observe high winds with a fetch of more than 500 km for which speed and the "from-which" direction remain statistically constant. The confidence that these vectors are suitable candidates for testing the above stated hypothesis is greatly increased, especially when there are actual buoy or ship reports in the area that agree well with the isobaric analysis.

The central pressures and isobaric gradients in extratropical cyclones are a direct measure of their intensity. Applying boundary layer physics to these known properties can result in realistic estimates of the associated vector wind.

The Braer Storm of 9 to 11 January, 1993 is recorded as the deepest North Atlantic cyclone of this century. The storm developed as a complex wave on January 9 and moved north eastward between NW Scotland and Iceland on January 10. It satisfies the definition of a meteorological "bomb". The 1200 GMT NMC analysis shown is Figure 3 estimates a central pressure of about 914 mb. As a further reference, Figure 4 shows the UK Met. Office surface analysis for the same synoptic time. Both maps exhibit good agreement and are mainly characterized by very strong gradients surrounding the low pressure of the storm. It is also important to point out that even at distances 10 to 12 degrees of latitude south from the center, there are winds measuring at least 50

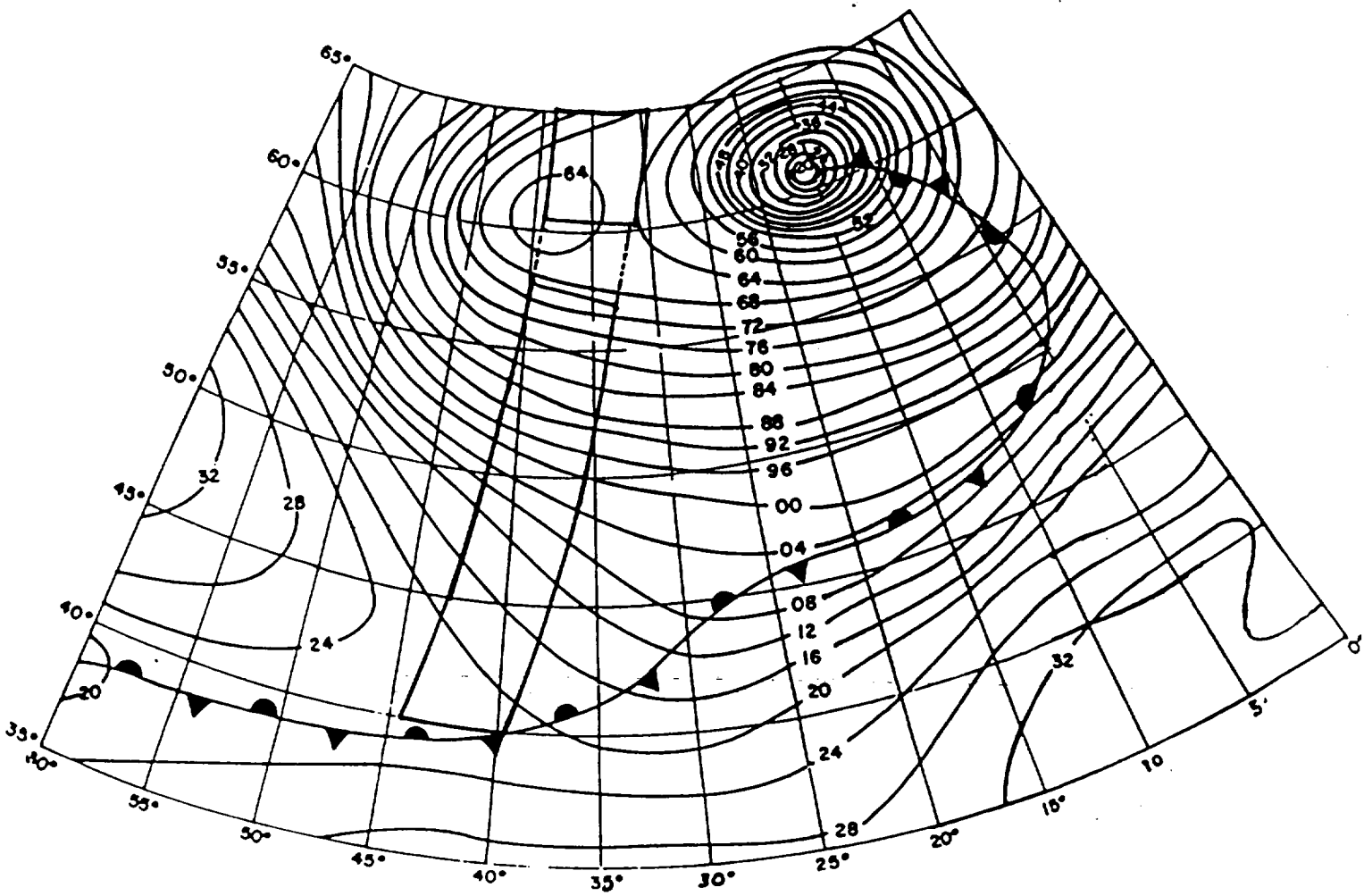

FIGURE 3. Final NMC Analysis: 1200Z Sunday 10, January 1993 The Well-Developed Braer Storm straddling the North Atlantic showing a dual low system with central pressures of less than 964 mb. and 920mb. respectively. The inset is a portion of the ERS-1 swath for Orbit No. 7796, Ascending Node 146.7, Southbound.

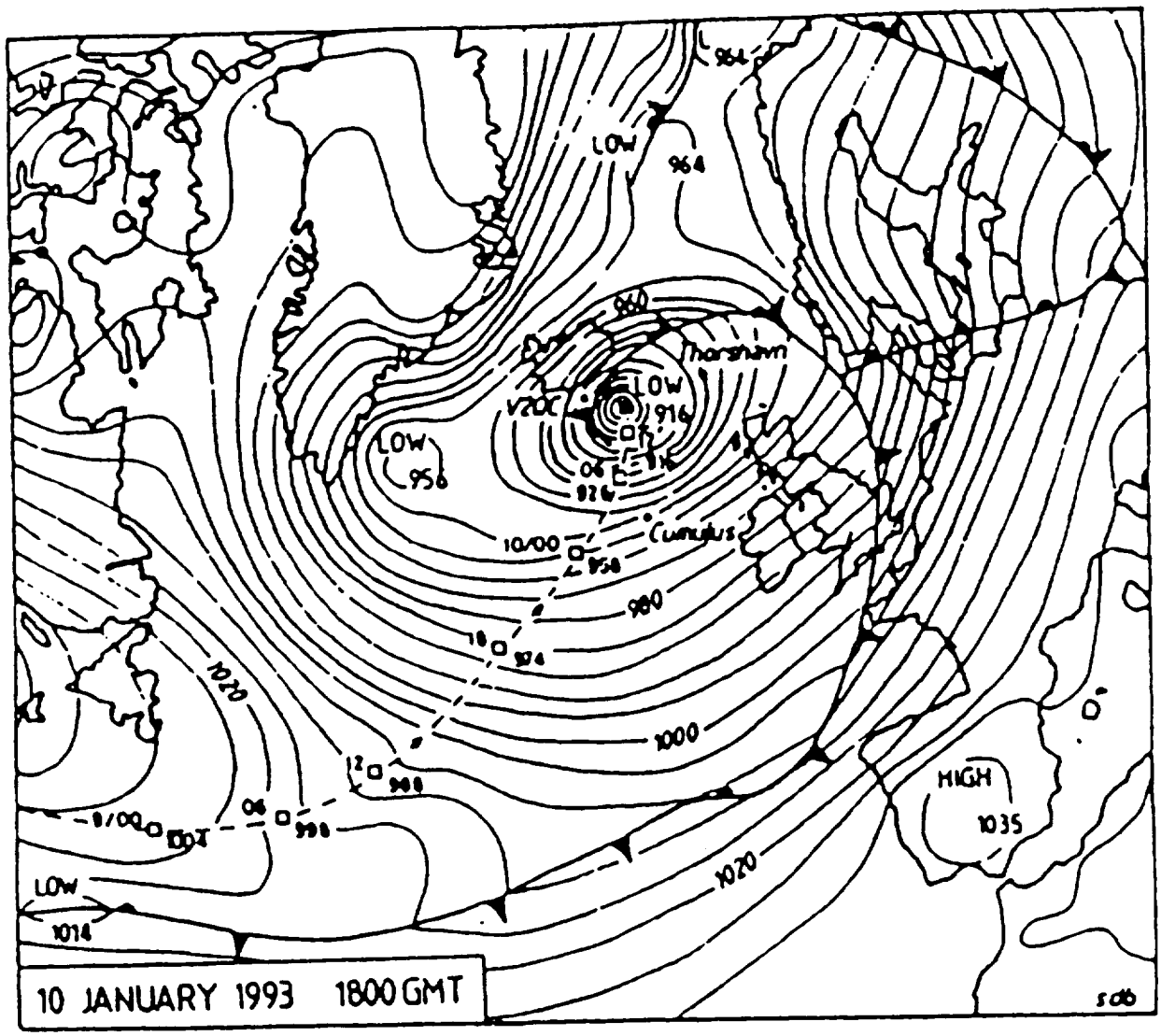

FIGURE 4.
Atlantic Surface Analysis at 1800 GMT, Jan 10, 1993 showing cyclone track and central pressure (mb) at 6-hour intervals. Isobars are drawn every 4 mbar. Courtesy of Stephen Burt, Mortimer, Berkshire

knots.

In general, data gathered from actual ships, data buoys and coastal stations showed winds in excess of 50 knots (25.7 m/s). Some reports were between 60 and 70 knots (30.84 and 35.98 m/s) with gusts to about 80 knots (41.12 m/s). There were also gusts in excess of 100 knots (51.4 m/s) reported by the UK Met. Office at particular stations.

The following are observations related to the Braer Storm in the North Atlantic.

Pressure:

Lowest Pressure (62° N 15° W)	912 - 915 mb
Buoy 44768 (60.8° N 19.4° W)	Pressure 930.4 mb [18 GMT Jan. 10] Pressure fall of 47 mb in 12 hr.
Ship V2QC (63.2° N 17° W)	Pressure 934.5 mb [15 GMT Jan. 10] Pressure fall of 42 mb in 12 hr.
Ocean Weather Ship Cumulus	Pressure fall in excess of 24 mb in 3 hr.
Area around 61° N 17° W	Pressure fall of 60 mb in 12 hr.

Winds:

- Strongest winds were confined to within about 280 km of the storm center.
- The geostrophic wind was estimated well in excess of 100 knots (51.4 m/s).
- Reported surface winds ranged from 50-70 knots (27.5 - 35.98 m/s).
- A gust of 105 knots (53.97 m/s) was measured at Roma, North Scotland.

The storm area experienced sustained high wind which are shown by the time series of the vector winds for three stations in Figure 5. In particular, Ocean Weather Ship Cumulus shows sustained wind in excess of 50 knots for the period 0300 to 1800 GMT on January 10. Figure 6 is

FIGURE 5. Abbreviated Weather Reports for Two Ships and a Station at Thorshavn in the Faeroe Islands. A Flag Represents 50 Knots. A Full Feather is 10 Knots and a Half Feather is 5 Knots. The Numbers on the Upper Right are the Atmospheric Pressure. For Example, 804 Represents 980.4 mb. The Upper Left is the Air Temperature. Thorshavn is at 62° 01'N, 6° 46'W. The Weather Codes, Where Shown, are From the WW Group in the Reports.

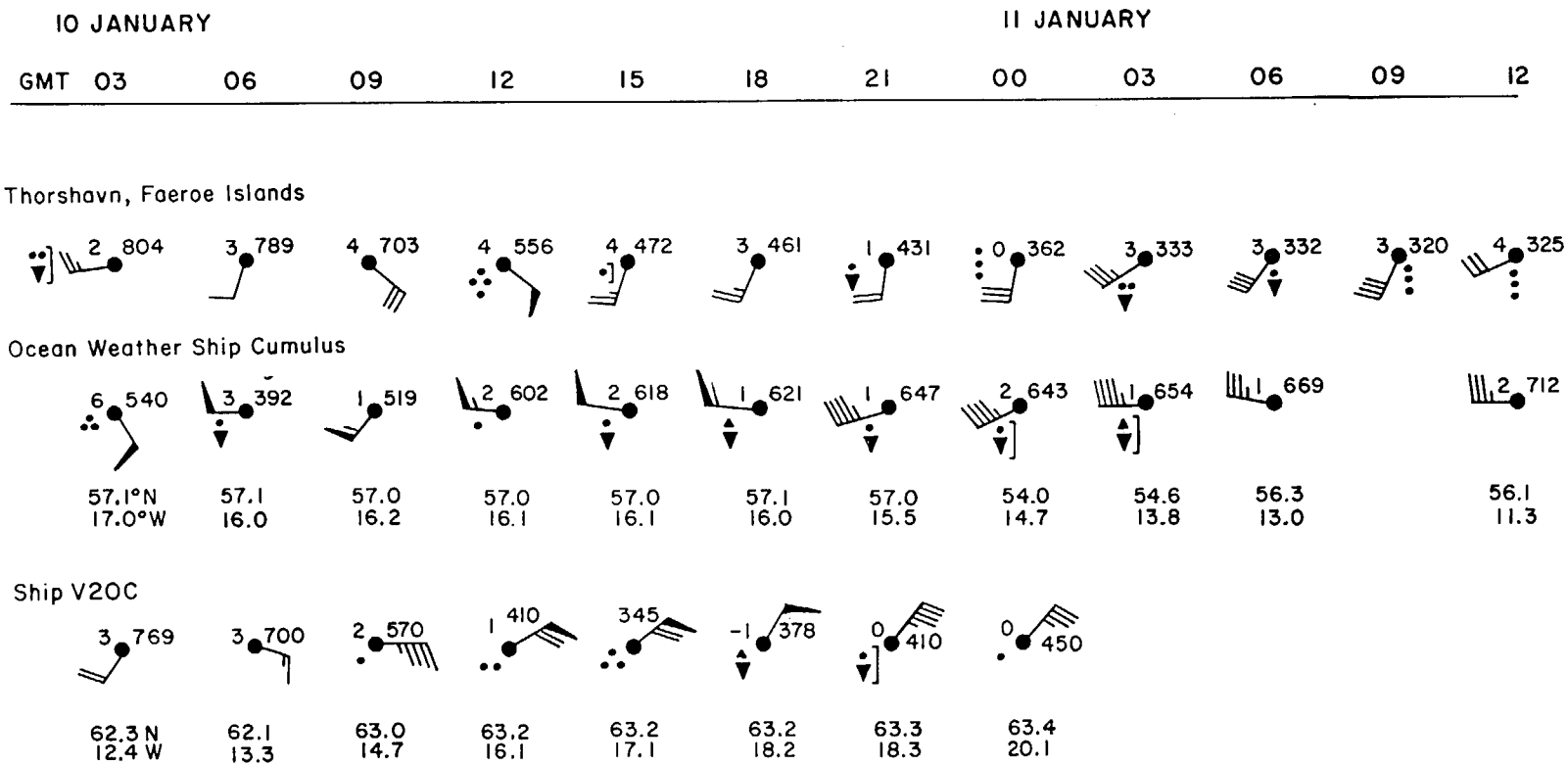

FIGURE 6. Examples of Measured Winds From Ships Associated with the Braer Storm. Wind Barbs are in kt.

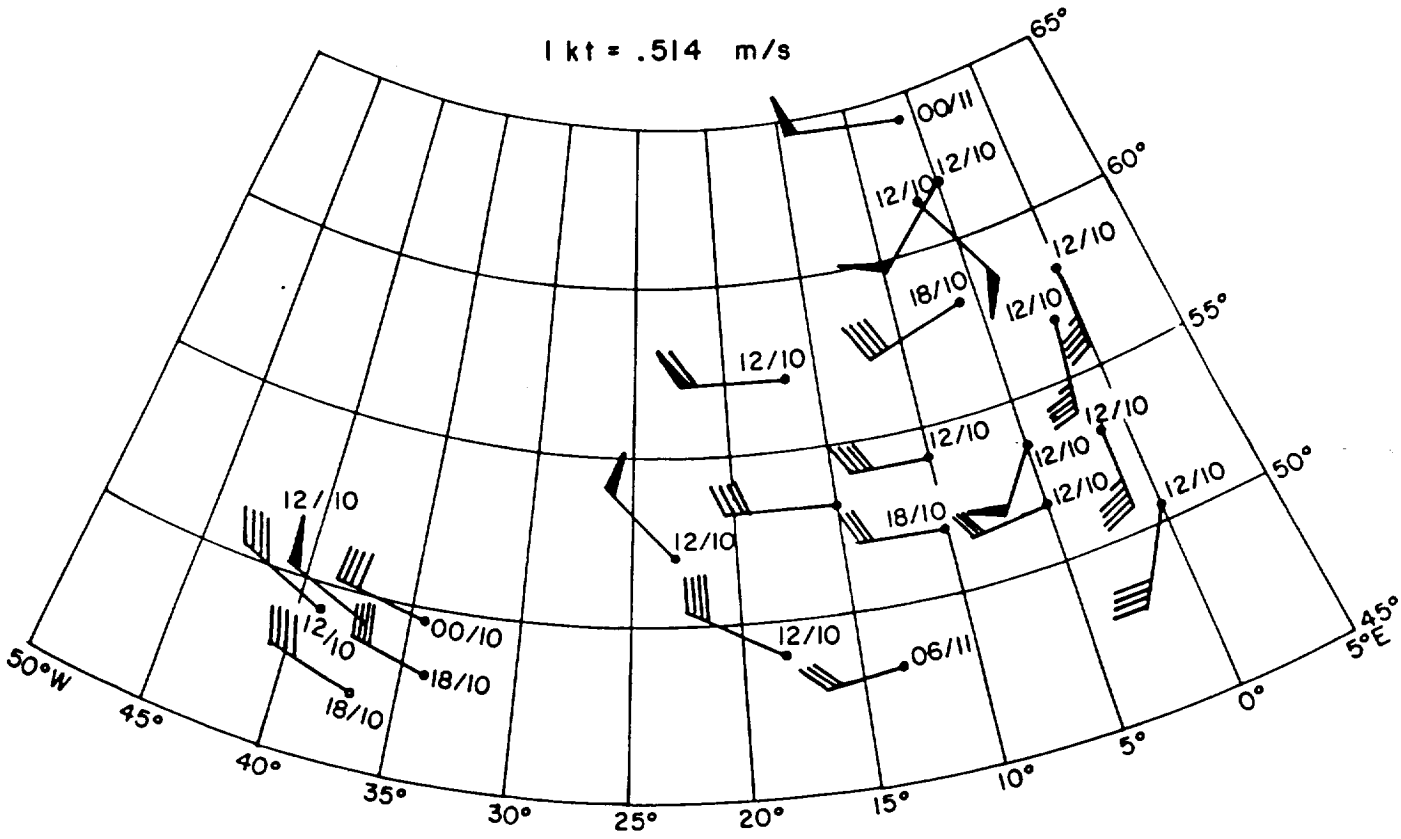

a summary of measured winds for the synoptic times given by (times/date).

As outlined earlier, products of the calculated winds from the pressure field can be mixed carefully with quality-controlled conventionally measured winds to produce a wind field against which satellite data can be compared.

The high wind case has not been completely analyzed. On the one hand, the PBL models have been difficult to get. After securing particular versions of them, they needed to be reprogrammed and updated. On the other, the greatest disappointment came when, in searching through the ERS-1 tapes, it was found out that data over the Braer Storm was sketchy at best and at most times, non-existent. There were many large gaps in the σ^0 data as the AMI was turned off at various points along the satellite track. However, the pass for Figure 3 has some data that can be used.

Empirically Determined Models

It is most important to have a better understanding of the basic functional form of the relationship between σ^0 and the wind vector. One simple method is to plot a scatter of wind speed versus σ^0 for a given incidence angle and wind direction. This has been tried often, but the results have not produced consistent results as shown by the many candidate models. There has been too much scatter in these plots and the regression equations have been inconsistent.

In an area of steady wind, that is, an area in the satellite swath where wind direction and speed are invariant over all 19 cells in the 500 km. across-track region, a model function can be treated in ways to provide a simplified relationship between σ^0 and the wind vector. The wind is allowed to change in the direction along track.

The Braer Storm provides a suitable candidates for this study. The assumptions

a) that the wind does not change by very much in direction or speed across the width of the swath and

b) that the wind only changes in the along track direction, should hold if meaningful results are to be obtained.

As an example, Figure 7 describes a portion of the Braer Storm in which the marked area is covered by the footprint of AMI-ERS-1 orbit for Jan. 11 1993. As this is a northbound pass, the winds are blowing parallel to the aft antenna. In this configuration, value returned by the aft antenna are related to downwind and those by the fore antenna are at or near cross-wind.

At each of the 19 cells in the cross track direction, the σ^0 value and wind speeds are stratified according to incidence angle. This being accomplished the simple relationship associating σ^0 with V can now be tested.

AMI and σ^0 Values

The AMI is a 5-cm active microwave instrument that measures the radar backscatter from the ocean surface. The capillary waves are the dominant transponders.

AMI's 3-antenna system is necessary to resolve the directional portion of the wind vector. A schematic of the antenna geometry is given in Figure 8 adopted from *Gemmill et al,* (1994), NOAA. This well-illustrated diagram highlights important information relating to sigma-0 and the antenna configuration. The figure depicts the antenna orientation for a northbound pass. A wind blowing parallel to, but opposite to the forward direction of an antenna is designated as upwind. When it blows just parallel to and in the same direction of advance of the antenna, it is labelled as

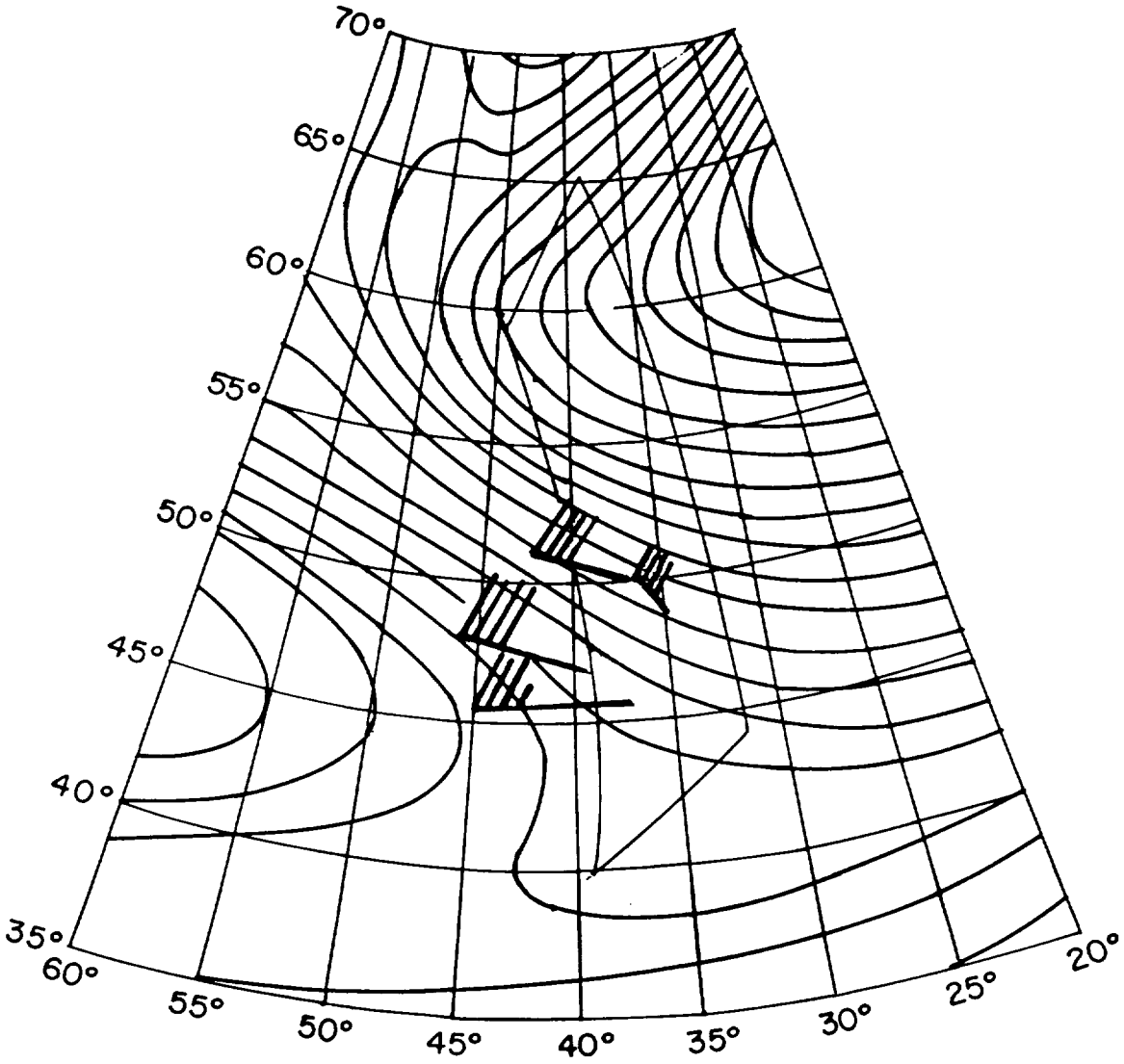

FIGURE 7 . NMC Final Surface Analysis 0000 GMT 11 January. Isobars Describe the Western Half of the Braer Storm. The inset is the Area Covered by the Footprints of AMI ERS-1 Orbit for 11 January 1993, Asc. Node 330.7 Long. 00:27 GMT. The Inset Also Defines the Study Area.

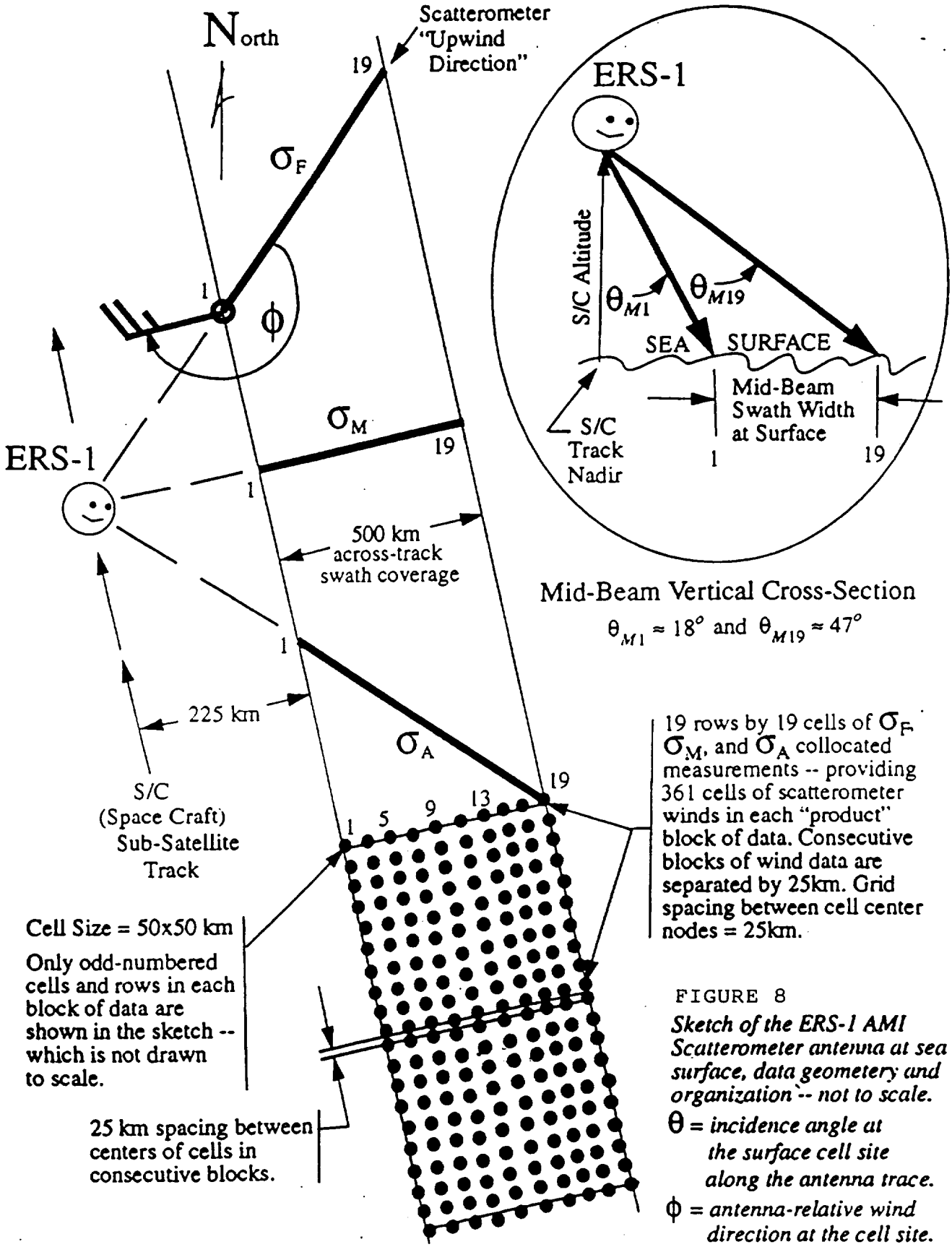

FIGURE 8

Sketch of the ERS-1 AMI Scatterometer antenna at sea surface, data geometery and organization -- not to scale.

θ = *incidence angle at the surface cell site along the antenna trace.*

ϕ = *antenna-relative wind direction at the cell site.*

(Adopted From Gemmill, et al. 1994).

downwind. Crosswind is near 90° to upwind or downwind.

The methodology outlined in the section on Method and Material has been utilized to process the wind field for an area of the Braer Storm that coincided with the footprints of AMI (marked in Figure 7). The NMC synoptic map for January 11 at 0000Z shows strong winds north of 45°N.

Actual ship reports in the vicinity of latitudes 45°N to 50°N are for 40 knots (~ 20 m/s). The gradients north of this area are tighter and therefore suggest the existence of winds in excess of 50 knots (~ 25 m/s). The wind array on which calculations and conlusions are based in this report was arrived at after processing and reanalysis that incorporated the following information data bases and meteorological models and practices.

- NMC final analysis 11 January, 0000Z.
- Actual ship reports.
- Information from the Braer Storm (UK Met. Office).
- Cardone's methodology (Refer to Table 1).
- ERS-1 AMI scatterometer wind and sigma-0 products (JPL).

Figure 9 shows a histogram of JPL wind speeds for the study area. Attention is directed to the calculated mean of 13.8 m/s. When compared with data from the other sources, it is seen that the product from JPL underestimated the representative winds by 5 to 7 m/s.

Winds of about 26 m/s were detected in the array. Wind magnitude at discrete points in the array served as the input values to the empirically determined model.

Some interesting and informative plots emerged. As examples, Figures 10 and 11 are presented in this report as part of our preliminary results. The plots are for incidence angles 38° and 42°. The top graphs are the regression lines predicted by Eqns. (11) and (12) that follow. From

FIGURE 9. Histogram of JPL Wind Speeds

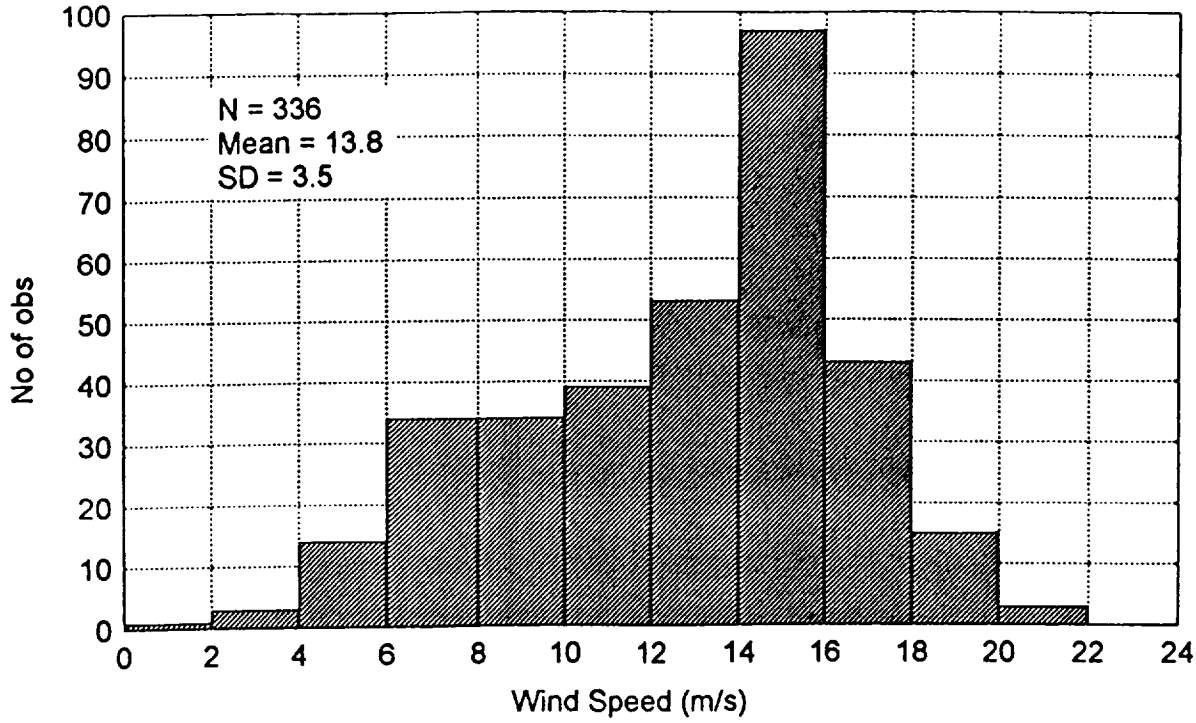

AMI- ERS Footprints for Orbit Jan 11, 1993, Asc. Node 330.7 Long 00:27GMT
(A Segment in Study Area)

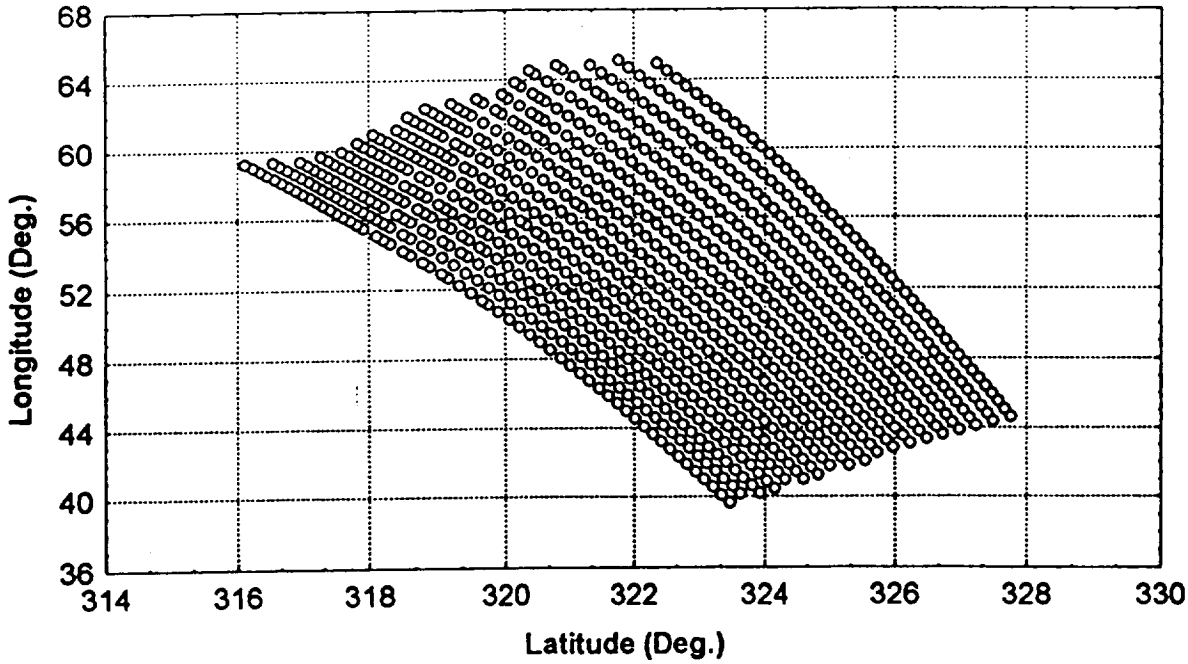

these two lines an estimate for upwind can be made as given in Eqn. (13).

The bottom Figures (10b, 11b) highlight the relationship between sigma-0 (max) and sigma-0 (min). The slight scatter about the regresssion line is an indication that this empirical model may produce some useful results. This statement is made in light of similar plots made in earlier studies by *Sylvester, et al.* (1989, 1990). Those max-min plots show the awesome scatter of the data. The points scatter from an outer edge all the way down to the 45° line. In the present plots points are concentrated at the outer edges only.

Although the results are somewhat premature, they are, however, encouraging. It appears from this study that the AMI scatterometer can detect winds that are in excess of 20 m/s. In this case winds are detected as high as 26 m/s.

The derivation of an empirical model for high winds follows.

The model proposed by *Long* (1985) with an additional $\cos 3\chi$ term is given by

$$\sigma^0(v, \chi, \theta) = U(1 + b_1 \cos \chi + b_2 \cos 2\chi + b_3 \cos 3\chi)/(1 + b_1 + b_2 + b_3)$$

where

$$\log_{10} U = 1.877 - 0.1466 \cos \theta + 0.00105 \theta^2 + \gamma \cdot \log_{10} V$$

and $\gamma = 0.09885 - 0.506 \theta - 0.000406 \theta^2$

For upwind, this become

$$\sigma^0(v, \chi, \theta) = U = F(\theta) V^{\gamma(\theta)}$$

This model is a simple power law as described previously. The partial derivative of σ^0 with respect to χ is zero at $\chi = 0$ (upwind) and at $\chi = 180°$ (downwind) so that the model is slowly varying with χ for these two directions.

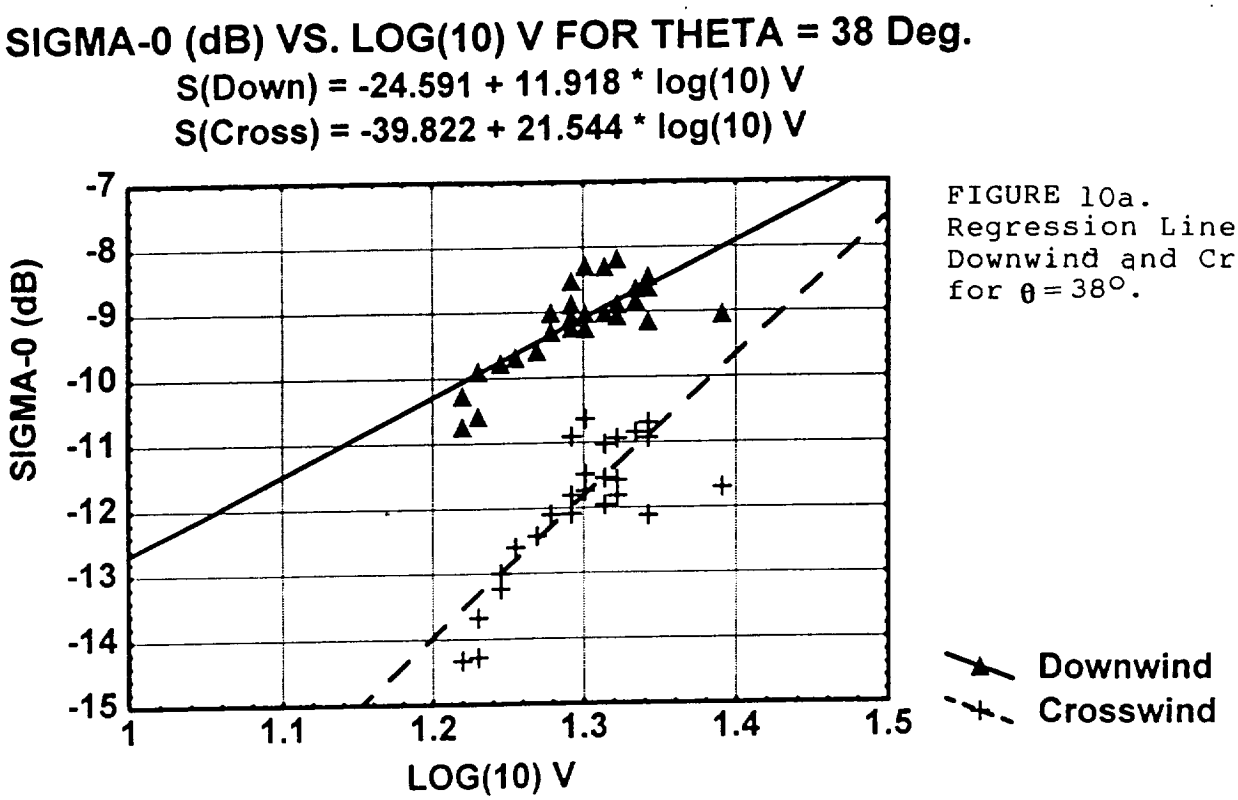

FIGURE 10a.
Regression Lines for Downwind and Crosswind for $\theta = 38^{o}$.

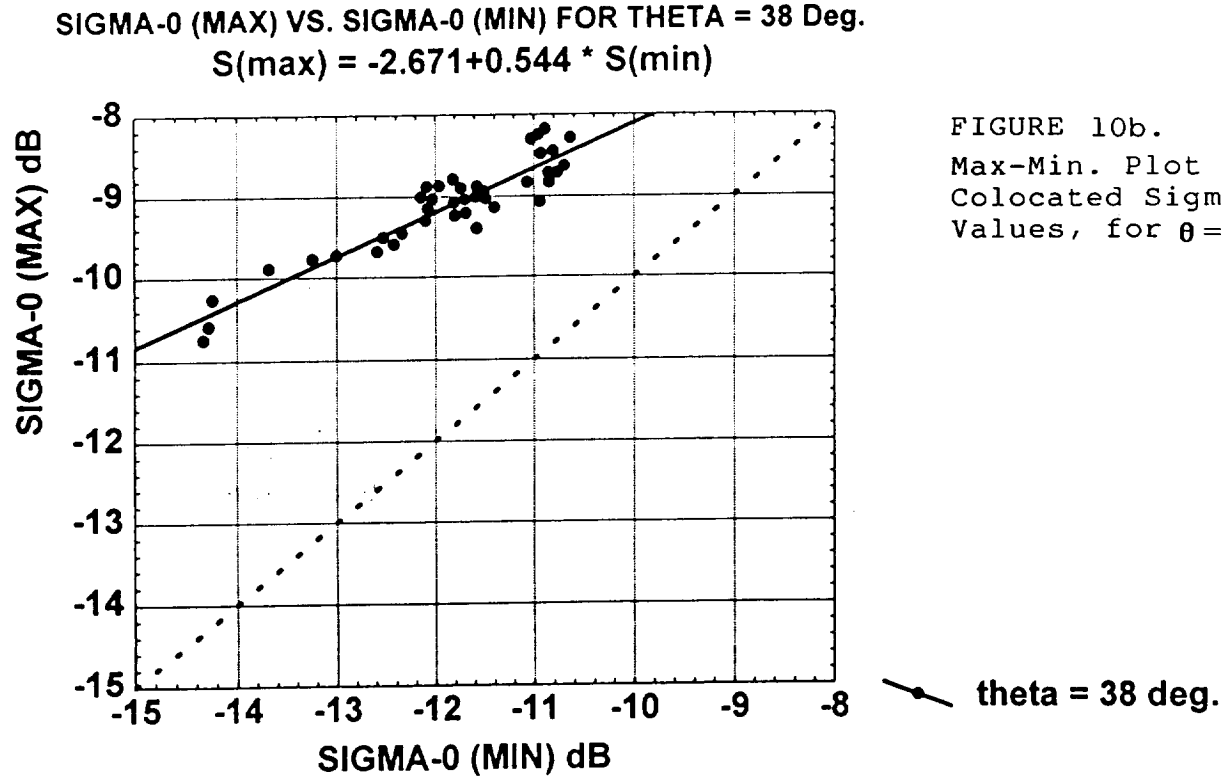

FIGURE 10b.
Max-Min. Plot for Colocated Sigma-O Values, for $\theta = 38^{o}$.

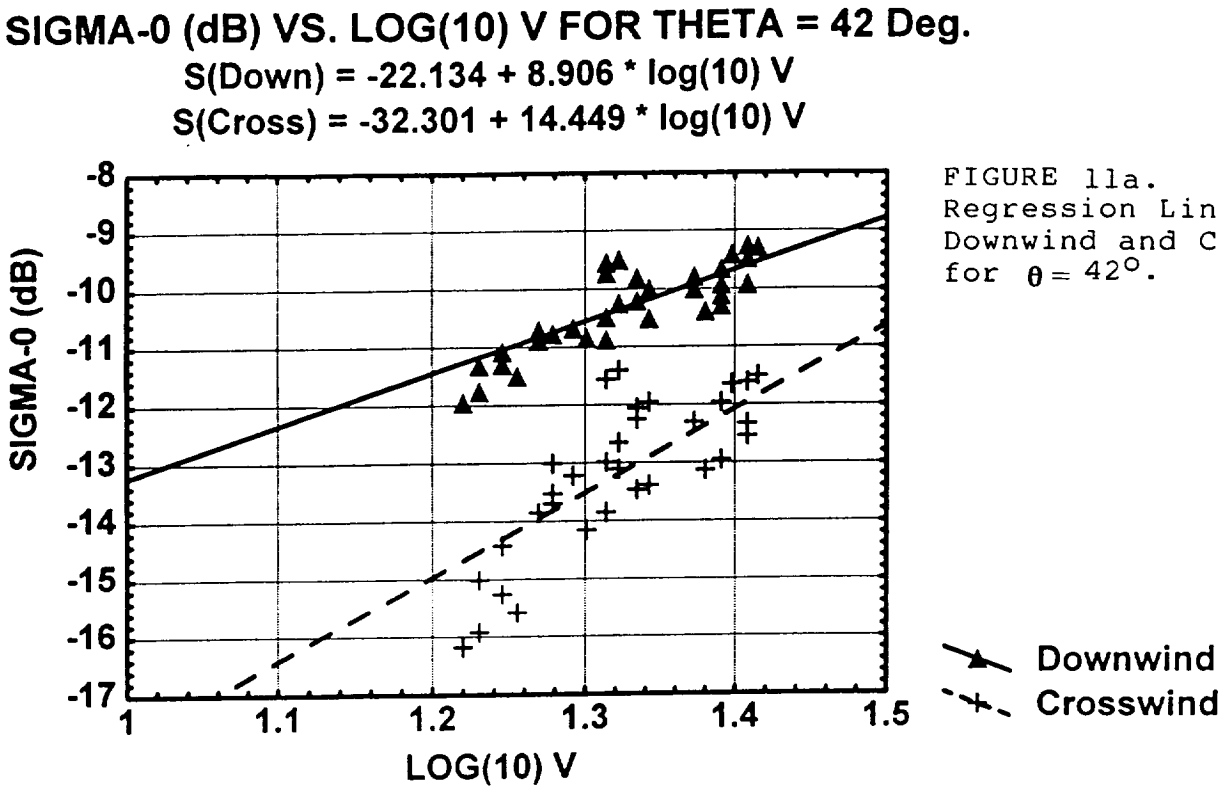

FIGURE 11a.
Regression Lines for Downwind and Crosswind for $\theta = 42^{o}$.

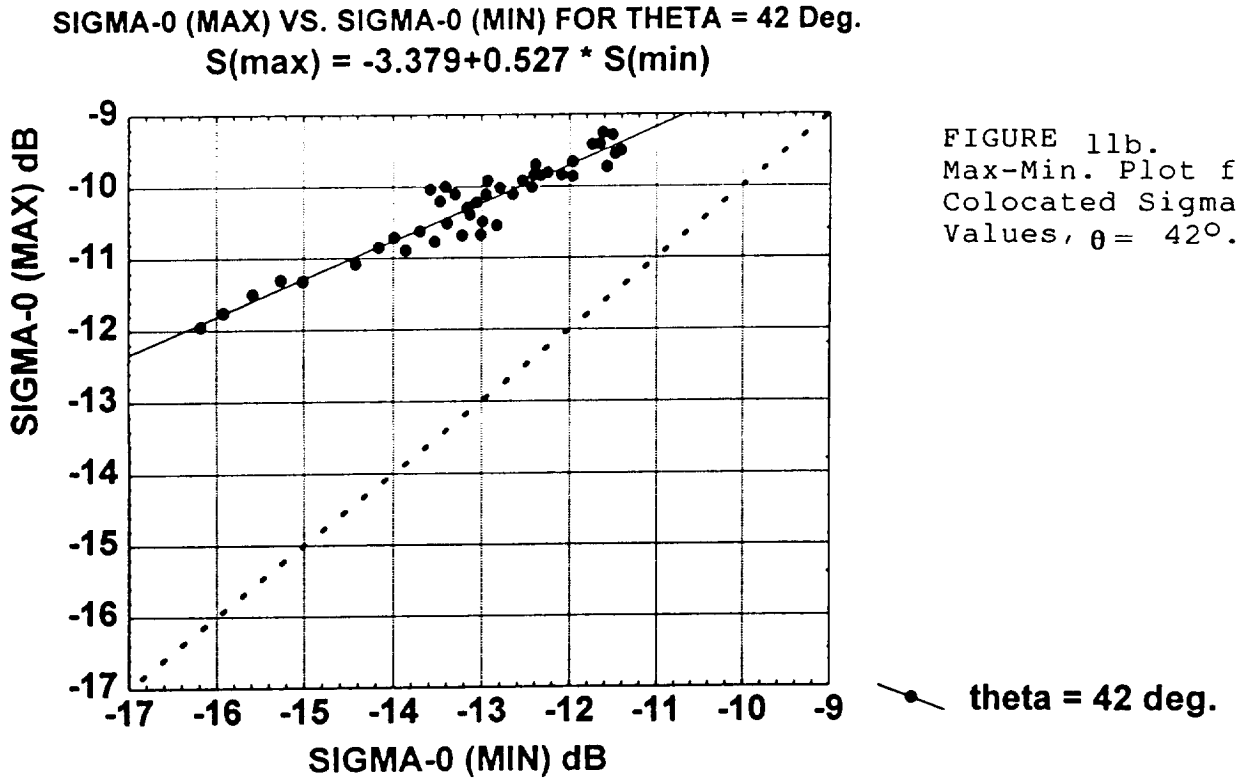

FIGURE 11b.
Max-Min. Plot for Colocated Sigma-0 Values, $\theta = 42^{o}$.

At downwind, Eqn. becomes

$$\sigma^0(v, 180^o, \theta) = F(\theta)\, V^{\gamma(\theta)} R$$

where

$$R = (1 - b_1 + b_2 - b_3)/(1 + b_1 + b_2 + b_3)$$

For vertical polarization, the downwind upwind ratio is slightly less than one.

Thus Braer Storm backscatter and wind speed data for the swath shown in Figure 7 for a line perpendicular to the track is very close to downwind for the aft antenna and close to crosswind for the fore antenna.

A preliminary evaluation of the winds in this swath can be paired with backscatter values for each row of cells at constant θ so as to obtain estimates of $F(\theta)$ and $\gamma(\theta)$. The values for $F(\theta)$ and $\gamma(\theta)$ given by *Long* (1985) yield results that are not consistent for the high winds in the Braer Storm so that it will be necessary to find new values for these two functions for each row of cells parallel to the subsatellite track.

These figures show that the backscatter values in the data occur at the outer edge of the plots originally obtained from the SEASAT data as in *Sylvester, et al.* (1989, 1990). This means that the downwind values and crosswind values can be estimated from the regression lines.

Thus in base 10,

$$\log \sigma_C^o = G_C + H_C \log V \qquad (11)$$

$$\log \sigma_D^o = G_D + H_D \log V \qquad (12)$$

An estimate from upwind would be

$$\log \sigma_U^o = G_U + H_U \log V \tag{13}$$

where G_U would be slighly larger than G_D, and H_U would be slighly less than H_D.

The subscripts U, D and C refer to upwind, downwind and crosswind.

As an extention of the results of Pierson given in the report by the model function subcommittee let,

$$\sigma_B^o = \log \sigma^o = (A_0 + A_1 \cos \chi + A_2 \cos 2\chi + A_3 \cos 3\chi) + (B_0 + B_1 \cos \chi + B_2 \cos 2\chi + B_3 \cos 3\chi) \log V \tag{14}$$

where σ_B^o is in bels and where $A_3 = A_1/3$ and $B_3 = B_1/3$ ensures that the minima of $\log\sigma^o$ will be at 90° and 270°.

By requiring that Eqn. (14) reduces to Eqns. (11), (12) and (13), the result is

$$A_0 = (G_U + G_D)/4 + G_C/2 \tag{15}$$

$$A_1 = 3 (G_U - G_D)/8 \tag{16}$$

$$A_2 = (G_U + G_D)/4 - G_C/2 \tag{17}$$

$$A_3 = (G_U - G_D)/8 \tag{18}$$

and

$$B_0 = (H_U + H_D)/4 + H_C/2 \tag{19}$$

$$B_1 = 3 (H_U - H_D)/8 \tag{20}$$

$$B_2 = (H_U + H_D)/4 - H_C/2 \tag{21}$$

$$B_3 = (H_U - H_D)/8 \tag{22}$$

Eqns. (11), (12) and (13) can be converted to natural units as in

$$\sigma_U^o = \alpha_U V^{\beta_U} \tag{23}$$

$$\sigma_C^o = \alpha_C V^{\beta_C} \quad (24)$$

$$\sigma_D^o = \alpha_D V^{\beta_D} \quad (25)$$

Let

$$\sigma_N^o = \alpha V^{\beta} \quad (26)$$

where

$$\alpha = \alpha_0 + \alpha_1 \cos \chi + \alpha_2 \cos 2\chi + \alpha_3 \cos 3\chi \quad (27)$$

$$\beta = \beta_0 + \beta_1 \cos \chi + \beta_2 \cos 2\chi + \beta_3 \cos 3\chi \quad (28)$$

and $\alpha_3 = \alpha_1/3 = \beta_3 = \beta_1/3$ (29)

Then $\alpha_0 = (\alpha_U + \alpha_D)/4 + \alpha_C/2$ (30)

$$\alpha_1 = 3(\alpha_U - \alpha_D)/8 \quad (31)$$

$$\alpha_2 = (\alpha_U + \alpha_D)/4 - \alpha_C/2 \quad (32)$$

$$\alpha_3 = (\alpha_U - \alpha_D)/8 \quad (33)$$

and $\beta_0 = (\beta_U + \beta_D)/4 + \beta_C/2$ (34)

$$\beta_1 = 3(\beta_U - \beta_D)/8 \quad (35)$$

$$\beta_2 = (\beta_U + \beta_D)/4 - \beta_C/2 \quad (36)$$

$$\beta_3 = (\beta_U - \beta_D)/8 \quad (37)$$

The graphs of these two forms for a model when plotted in either natural or logarithmic form will only be the same at $\chi = 0°$, $\chi = 90°$ and $270°$. For any value of the wind speed, for example for

$$10^{\log \sigma_B^o} = \sigma_N^o \quad (38)$$

The graphs will be the same as V is varied at upwind, crosswind and downwind for any θ, but for other values of χ they will differ. This property could yield improved values for the variation with wind direction by using either

$$\sigma_B^{\circ} = \log \sigma^{\circ}_{(combined)} = K\, \sigma_B^{\circ} + (1 - K) \log \sigma_N^{\circ} \quad \text{for } 0 < K < 1 \tag{39}$$

on a logarithmic scale or as

$$\sigma_N^{\circ}{}_{(combined)} = K\,(10^{\sigma_B^{\circ}} + (1 + K)\sigma_N^{\circ} \quad \text{for } 0 < K < 1 \tag{40}$$

on a scale with natural units.

REVIEW OF OCEANOGRAPHIC RESEARCH AND NASA GRANTS

The National Aeronautics Space Administration and the Jet Propulsion Laboratory have been the principal supporters of research at The City College since September 1973 along with a number of smaller grants and contracts from other sources. Prior to that, support was provided at New York University even before Skylab was put into orbit.

Prior to that at NYU, Professors Gerhard Neumann and Willard J. Pierson Jr. were supported by the Office of Naval Research from about 1950 to 1965.

It is pertinent in this final report to review the contributions to the subject of remote sensing that were made over the period of time from about 1949 to the present. Hundreds of scientists all over the world are using and improving upon the results first obtained by this research.

However, research is always open ended. There are substantial areas where the present models and theories are inadequate. There are ways to improve on these models and theories. Much more still needs to be done.

NASA has supported this research since 1965. The current series of grants from NASA began on December 1, 1986 for a total funding of $754,000.00 (NAGW-690). The present series of grants from the Jet Propulsion Laboratory began on August 20, 1986 for a total funding extended until December 31, 1995 of $673,999.00. The number of people supported at various times has varied. Many have moved on to do research at various NASA activities or as contractors to NASA and other sources of support.

During the above time frame, this research has yielded a number of "firsts" all of which have had a profound effect on the present status of remote sensing. Some of them are listed chronologically below with a brief note on their impact to the subject.

Pierson, W. J. (1951): The interpretation of crossed orthogonals in wave refraction phenomena. Beach Erosion Board Tech. Memo. 21. **The effects of wave refraction over the continental shelf made it difficult to hindcast waves for the Beach Erosion Board using the Sverdrup Munk method to calculate the significant wave height and period.**

Pierson, W. J. (1951): On the propagation of waves from a model fetch at sea. Gravity Waves, NBS Circular 521, 175-186. **The first attempt to study the dispersion of waves.**

Pierson, W. J. (1952): A unified mathematical theory for the analysis, propagation, and refraction of storm-generated ocean surface waves. Parts I and II. College of Engineering, Res. Div., N.Y.U. **Never published but in the gray literature. Linear superposition of Airy Waves. (See Kinsman 1965).**

Pierson, W. J. and W. Marks (1952): The power spectrum analysis of ocean-wave records. Trans. Amer. Geophys. Un., 33, 6, 834-844. **This is the first paper ever published that showed how an ocean wave time history could be analyzed so as to resolve the total variance of the record into frequency bands. Spectra based on this result, as modified, are being routinely estimated from hundreds of wave records every day.**

St. Denis, M. and W. J. Pierson (1953): On the motions of ships in confused seas. Trans. Soc. Naval Architects and Marine Engineers, 61, 280-357. **This paper revolutionized the study of ship motions in random waves. Papers that use this study appear routinely in the Naval Architecture Literature, but it is so well know that few of them refer to it as the source. The 1973 "Certificate of Appreciation" noted that the paper "Changed our thinking about the ship, the sea, and the ship upon the sea". Important papers on bow submergence and slamming, ship routing and data analysis of ship trials resulted from this paper. The theory is "linear". Efforts to do the nonlinear problem are presently under way.**

Pierson, W. J. (1955): Wind-generated gravity waves. Advances in Geophysics, 2, 93-178. Academic Press. New York. **Defined waves as a stochastic process that still satisfied the linearized wave equations.**

Pierson, W. J., G. Neumann and R. W. James (1955): Practical methods for observing and forecasting ocean waves by means of wave spectra and statistics. H. O. Pub. 603, U.S. Navy Hydrographic Office, Washington, DC. **The first attempt to forecast wave spectra. The book is still used at the United States Naval Academy.**

Pierson, W. J. (1960): (Editor and co-author) The directional spectrum of a wind-generated sea as determined from data obtained by the Stereo Wave Observation Project, by Cote et al., Meteor. Papers, 2, 6, New York University Press, N.Y. **The first directional wave spectrum based on a linear model. See the books by Kinsman (1965) and Neumann and Pierson (1965).**

Pierson, W. J. and J. F. Dalzell (1960): The apparent loss of coherency in vector Gaussian processes due to computational procedures with application to ship motions and random seas. Sci. Rept. under Contr. Nonr. 285(17) and 263(09), College of Engineering, Res., Div., N.Y.U. **Introduced the concept of co and quadrature spectra to the study of ship motions.**

Pierson, W. J. (1964): The interpretation of wave spectrums in terms of the wind profile instead of the wind measured at a constant height. J. Geophys. Res., 69, 24, 5191-5203. **The variation of wind with height needs to be considered in wave forecasting.**

Pierson, W. J. and L. Moskowitz (1964): A proposed spectral form for fully developed wind seas based on the similarity theory of S. A. Kitaigorodskii. J. Geophys. Res., 69, 24, 5181-5190. **This proposed spectral form is still used to model fully developed seas. A paper in the 1994 Transactions of the Society of Naval Architect and Marine Engineers found that this spectrum fitted very high waves data very well.**

Neumann, G. and W. J. Pierson (1966): Principles of Physical Oceanography. Prentice Hall, Englewood Cliffs, New Jersey. **Provided the background on wave theory and wave forecasting up to the time of publication.**

Pierson, W. J., L. J. Tick and L. Baer (1966): Computer based procedures for preparing global wave forecasts and wind field analyses capable of using wind data obtained by a spacecraft. Sixth Naval Hydrodynamics Symps., Sept. 28, Oct. 4, 1966. **Described the numerical spectral wave forecasting model used at the Fleet Numerical Oceanographic Center for many years. Some changes have been made.**

Greenwood, J. A., A. Nathan, W. J. Pierson, G. Neumann, F. C. Jackson and T. Pease (1969a): Radar altimetry from a spacecraft and its potential applications to geodesy. Remote Sensing of Environment, 1, 59-70. **The first paper to propose radar altimetry. Compared the widely different results for the geoid over the oceans and showed how a radar altimeter could measure the geoid.**

Greenwood, J. A., A. Nathan et al., (1969b): Oceanographic applications of radar altimetry from spacecraft. Remote Sensing of Environment, 1, 71-80. **Showed that a radar altimeter could measure the slope of the ocean across the Gulf Stream, tides, storm surges and tsunamis. All of the predictions of these two papers have been verified far beyond those that were made at that time with the exception of measuring tsunamis. Advancing technology has produced increasingly more accurate altimeters.**

Moore, R. K. and W. J. Pierson (1971): Worldwide oceanic wind and wave predictions using a satellite radar- radiometer. J. Hydronautics, 5, 2, April, 52-60. **A prediction (somewhat incorrect) of the future.**

Pierson, W. J. and R. K. Moore (1972): A proof of concept test of a method for determining the wind and pressure fields in the planetary boundary layer and measuring wave height over the ocean by means of a combination radar-passive microwave-altimeter on SKYLAB. Published by WMO as a part of the Proceedings of a Technical Conference on the Means and Acquisition and Communication of Ocean Data. **A paper presented in Japan.**

Pierson, W. J., V. J. Cardone, and J. A. Greenwood (1974): The application of SEASAT-A to meteorology. The University Institute of Oceanography (now Remote Sensing Lab). Prepared for the SPOC group of NOAA/NESS Contract 04-4158-11. **The first paper to show that two backscatter values 90° apart could be used to recover both wind speed and wind direction with ambiguities. This result is the foundation of all of the present methods for recovering winds from backscatter data.**

Cardone, V. J., J. D. Young, W. J. Pierson, R. K. Moore, J. A. Greenwood, C. Greenwood, A. K. Fung, R. E. Salfi, H. L. Chan, M. Afarani and M. Komen (1975): The measurement of the winds near the ocean surface with a radiometer-scatterometer on SKYLAB. Final Report of EPN 550 Contr. No. NAS-9-13642, NASA Lyndon B. Johnson Space Center, Houston, Texas. **The analysis of the scatterometer data from S193 on SKYLAB was able to show that backscatter varied as a function of wind direction as demonstrated more conclusively by the AAFE Langley Circle Flights.**

Pierson, W. J., W. E. Marlatt, Z. H. Byrns and W. R. Johnson (1978): Oceans and atmosphere, in SKYLAB EREP Investigations Summary, NASA SP-399. National Aeronautics and Space Administration. U. S. Govt. Printing Office Stock No. 033-00-00741-8. 189-256. **The NASA SP-399 summarized the major results of the SKYLAB Earth Resources Experiment Package including the altimeter measurements over sea mounts and submarine trenches.**

Brown, R. A., V. J. Cardone, T. Guymer, J. Hawkins, J. E. Overland, W. J. Pierson, S. Peteherych, J. C. Wilkerson, P. M. Woiceshyn and M. Wurtele (1982): Surface wind analyses for Seasat. J. Geophys. Res., 87, C5, 3355-3364. **A detailed analysis of SEASAT data.**

Jones, W., L. C. Schroeder, D. H. Boggs, E. Bracalente, R. Brown, G. Dome, W. J. Pierson and F. J. Wentz (1982): The Seasat-A satellite scatterometer: The geophysical evaluation of remotely sensed wind vector. J. Geophys. Res., 87, C5, 3297-3317. **A detailed analysis of SEASAT data.**

Pierson, W. J. (1982): The spectral ocean wave model (SOWM), a Northern Hemisphere computer model for specifying and forecasting ocean wave spectra. David W. Taylor Naval Ship Research and Development Center. DTNSRDC-82/011. **The SOWM was the forerunner of all present computer based wave forecasting models. Modifications of it are used in Canada and the Fleet Numerical Weather Center.**

Schroeder, L. C., D. H. Boggs, G. Dome, I. M. Halberstam, W. L. Jones, W. J. Pierson and F. J. Wentz (1982): The relationship between wind vector and normalized radar cross section used to derive Seasat-A satellite scatterometer winds. J. Geophys. Res., 87, C5, 3318-3336. **Documentation of the SEASAT winds.**

Pierson, W. J. (1983): The measurement of the synoptic scale wind over the ocean. J. Geophys. Res., 88, C3, 1683-1708. **Conventionally measured winds differ from the desired synoptic scale winds because of the duration of the average and mesoscale effects. There is a minimum root mean square difference between a backscatter wind and a conventionally measured wind even for perfect data.**

Pierson, W. J., W. B. Sylvester and R. E. Salfi (1984a): Synoptic scale wind field properties from the Seasat-SASS. CUNY Institute of Marine and Atmospheric Sciences. The City College of New York. Grant NAGW-266. NASA Contractor Report 3810.

Pierson, W. J., W. B. Sylvester and R. E. Salfi (1984b): Vector wind, horizontal divergence, wind stress and wind curl from Seasat-SASS at a one degree resolution. CUNY Institute of Marine and Atmospheric Sciences. The City College of New York, Proceedings of "Frontiers of Remote Sensing of the Oceans of Troposphere from Air and Space Platforms. URSI Commission F Symposium and Workshop. NASA Conference Publication 2303. Israel, May 14-23. 557-566. **A summary of the above contractor's report. The curl and divergence of the boundary layer wind can be calculated and confidence intervals on the values can be computed.**

Donelan, M. A. and W. J. Pierson (1987): Radar-scattering and equilibrium ranges in wind-generated waves - with application to scatterometry. J. Geophys. Res., 92, C5, 4971-5029. **This model for backscatter of L-band, C-band, X-band and K_u-band has some features that appear to be verified and other features that are incorrect. The effect of viscosity for capillary waves is important.**

Sylvester, W. B., W. J. Pierson and S. R. Breitstein (1989): Techniques for evaluating the performance of models of radar backscatter from the ocean surface: Suggestions for their improvement, *in*, IGARSS '89 Quantitative Remote Sensing: An Economic Tool for the Nineties, 5, 2291-2296. Library of Congress #89-84217, IEEE Catalogue No. #89 CH2768-0.

Sylvester, W. B., W. J. Pierson and S. R. Breitstein (1990): Further results on "techniques for evaluating the performance of models of radar backscatter from the ocean surface: Suggestions for their improvement" *in* IGARSS '90, Remote Sensing Science for the Nineties, *3*, Library of Congress 89-82170, Catalogue No. 90-CH2825-8, 2149-2156. **These two papers obtained a new way to compare different models for backscatter and showed that one of them utilized the data whereas the other two did not. Many unanswered questions were revealed by this study.**

Pierson, W. J. (1989a): Probabilities and statistics for backscatter estimates obtained by a scatterometer with application to new scatterometer design data. NASA Contractor's Report 4228, 123 p.

Pierson, W. J. (1989b): Probabilities and statistics for backscatter estimates obtained by a scatterometer. J. Geophys. Res., 94, C7, 9743-9759. **The above contractor's report contains greater detail. Negative values for the backscattered power were obtained by SEASAT but not understood. These papers explained why this happens and derived the confidence intervals on the measurements (estimates) of the backscatter. The maximum likelihood estimates for the recovered wind speeds and direction were derived in this paper and are used by JPL in recovering winds.**

Pierson, W. J. (1990): Examples of, reasons for, and consequences of the poor quality of wind data from ships for the marine boundary layer: Implications for remote sensing (1990): J. Geophys. Res., 95, C8, 13313-13340, August 13. **Close-by ship reports of wind speed and direction are compared to show how poorly winds are reported by these ships. Only data buoy winds can be used to validate scatterometer winds.**

Pierson, W. J. (1991): Comment on "Effect of sea maturity on satellite altimeter measurements" by Roman E Glazman and Stuart H. Pilorz. J. Geophys. Res., 96, C3, 4973-4977. **Some authors do not understand the complexity of the variability of wave spectra. A wind generated sea cannot have a wave age of 6 (or as more recently claimed 3).**

Pierson, W. J., M. A. Donelan and W. H. Hui (1992): Linear and nonlinear propagation of water wave groups. J. Geophys. Res., 97, C4, 5607-5621. **This paper showed that coalescing transient wave groups do not behave as the linear theory predicts. The Fourier integral spectrum changes from station to station as the transient propagates down the wave tank.**

Pierson, W. J. (1993): Oscillatory third-order perturbation solutions for sums of interacting long crested Stokes waves on deep water. Journal of Ship Research, 37, 4, 354-383. (Errata in J. Ship Res. 38, 2, p 136). **This paper is a major breakthrough in wave theory. It is just the start toward the solution of the difficult problem of finding a realistic stochastic description of nonlinear waves.**

Pierson, W. J. and L. J. Tick (1994): Experimental results for towing tank studies of nonlinear water waves. in Proceedings of the Symposium on the Air-Sea Interface Marseilles, France. (To be published by the University of Toronto Press). **A preliminary description of some experiments. The full report on these experiments is three quarters completed.**

REFERENCES

Blake, R. A. (1991): The dependence of wind stress in wave height and wind speed. J. Geophys. Res. 96, C11, 20531-20545.

Brown, R. A., and T. W. Liu (1982): An operational large-scale marine planetary boundary layer model. J. of Applied Meteorology, 20, 261-269.

Cardone, V. J. (1969): Specification of the wind distribution in the marine boundary layer for wave forecasting. New York University, School of Engineering and Science TR 69-1.

Cardone, V. J. (1978): Specification of prediction of the vector wind on the U. S. Continental Shelf for Application to an Oil Slick Trajectory Forecasting Program. Report to the NWS, NOAA, IMAS, City College, NY.

Donelan, M. A. (1980): The dependence of the aerodynamic drag coefficient on wave parameters, *in* Proceedings of the First International Conference on Meteorology and Air-Sea Interaction of the Coastal Zone. American Meteorological Society, Boston, Mass. , pp. 381-387.

Donelan, M. A. (1990): Air-sea interaction, *in* the Sea, Vol. 9. Ocean Engineering Science, Editd by B. LeMehaute and D. Hanes, John Wiley, New York, pp. 239-292.

Gemmill, W. H., P. Woiceshyn, C. Peters, and V. M. Gerald (1994): A preliminary evaluation of scatterometer wind transfer functions for ERS-1 Data. Technical Note, Ocean Products Center of NMC, NOAA.

Long, A. (1985): Towards a C-band radar sea echo model for the ERS-1 Scatterometer. Euro. Space Technology Center, (ESTEC).

Long, D. G. (1995): (Chair) Current Progress in K_u-Band Model Functions. NSCAT Project Office, Jet Propulsion Laboratory. NSCAT Science Working Team Subcommittee on Geophysical Model Function.

Peters. C. A., V. M. Gerald, P. M. Woiceshyn and W. H. Gemmill (1994): Operational processing of ERS-1 scatterometer winds: Technical Note, Ocean Products Center of NMC, NOAA.

Pierson, W. J. (1978): TWINDX: A planetary boundary layer model for the winds in extratropical and tropical ocean areas. Part 3 of a final report prepared for the Naval Environmental Prediction Research Facility, Contr. N00014-77-C-0206. CR 79-02.

Pierson, W. J. (1989a): Probabilities and statistics for backscatter estimates obtained by a scatterometer with application to new scatterometer design data. NASA Contractor's Report 4228, 123 p.

Pierson, W. J. (1989b): Probabilities and statistics for backscatter estimates by a scatterometer. J. Geophys. Res. 94, C7, 9743-9759.

Pierson, W. J. (1990): Examples of, reasons for, and consequences of the poor quality of wind data from ships for the marine boundary layer: Implications for remote sensing (1990): J. Geophys. Res., 95, C8, 13313-13340, August 13.

Smith, S. D. (1980): Wind stress and heat flux over the ocean in gale force winds. J. Phys. Oceanogr., 10, pp. 709-726.

Smith, S. D. (1988): Coefficients for sea surface wind stress, heat flux, and wind profiles as a function of wind speed and temperature. J. Geophys. Res., 93, pp. 15467-15472.

Stoffelen A. and Anderson, D. (1995): The ECMWF contribution to the characterisation, interpretation, calibration and validation of ERS-1 scatterometer backscatter measurements and winds, and their use in numerical weather prediction models. European Centre for Medium-Range Weather Forecasts, European Space Agency Contract Report.87 p.

Sylvester, W. B. (1984): A SEASAT SASS simulation experiment to quantify the errors related to a ± 3-hour intermittent assimilation technique. NASA Grant NAGW-266, Contractor Report 3799. CUNY Institute of Marine and Atmospheric Sciences at the City College, New York.

Sylvester, W. B., W. J. Pierson and S. R. Breitstein (1989): Techniques for evaluating the performance of models of radar backscatter from the ocean surface: Suggestions for their improvement, in, IGARSS '89 Quantitative Remote Sensing: An Economic Tool for the Nineties, 5, 2291-2296. Library of Congress #89-84217, IEEE Catalogue No. #89 CH2768-0.

Sylvester, W. B., W. J. Pierson and S. R. Breitstein (1990): Further results on "techniques for evaluating the performance of models of radar backscatter from the ocean surface: Suggestions for their improvements", in, IGARSS '90, Remote Sensing Science for the Nineties, 3, Library of Congress 89-82170, Catalogue No. 90-CH2825-8, 2149-2156.

FIGURES